Skin Friction of Micropiles Embedded in Gravelly Soils

Abdul Karim Elsalfiti

A Thesis

In

The Department

Of

Building, Civil and Environmental Engineering

Presented in Partial Fulfillment of the Requirements

For the Degree of Master of Applied Science at

Concordia University

Montreal, Quebec, CANADA

November 2011

CONCORDIA UNIVERSITY
School of Graduate Studies

This is to certify that the thesis prepared

By: ABDUL KARIM ELSALFITI

Entitled: SKIN FRICTION OF MICROPILES EMBEDDED IN GRAVELLY SOILS

and submitted in partial fulfillment of the requirements for the degree of

MASTER OF APPLIED SCIENCE (CIVIL ENGINEERING)

complies with the regulations of the University and meets the accepted standards with respect to originality and quality.

Signed by the final examining committee:

Dr. M. Elektorowicz Chair

Dr. G. J. Gouw Examiner

Dr. L. Tirca Examiner

Dr. A. M. Hanna Supervisor

Approved by _____
Chair of Department or Graduate Program Director

_____
Dean of Faculty

Date November 30, 2011

ABSTRACT

Skin Friction of Micropiles Embedded in Gravelly Soils

Abdul Karim Elsalfiti

Micropiles are small in diameter (less than 300 mm) cast-in-place replacement piles, composed of steel reinforcement and placed or injected grout. They can withstand axial (compressive/tensile) and lateral loads, and work as components in a composite soil/pile mass or as small-diameter substitutes for conventional piles. Micropiles are used as underpinning elements to enhance bearing capacity of existing foundations and prevent excessive settlements. They can also be used as foundations for new structures and land stabilization.

Micropiles are distinguished in providing innovative drilling and grouting techniques, which in return enhance load resistance. Reinforcement steel elements compromise to about 50 percent of the pile's volume and is considered to be the main load bearing element, while the grout serves to transfer the load to the surrounding soils.

To evaluate the skin friction of micropiles embedded in gravelly soils, a numerical model was developed using the geotechnical software program GEO5 for piles. The model was validated using existing field tests. Upon achieving satisfactory results, the model was used to generate 30 load tests that were performed on micropiles in three types of gravelly soils, ranging from Silty Gravel (GM) to Well graded Gravel (GW). Load-Displacement curves were then developed and carefully examined. The parametric factors and geotechnical properties that could affect the skin friction were examined in a detailed manner. Present capacities measured from the Load-Displacement curves were then compared with existing design equations proposed by Reese and

O’Neill, Hassan and O’Neill and Kulhawy. Based on all the information gathered, modifications to existing design equations were developed when needed to predict the skin friction for micropiles embedded in Gravelly Soils, while providing a marginal factor of safety.

ACKNOWLEDGEMENTS

I would like to express my sincere gratitude to my supervisor, Dr. Adel Hanna for his continuous support and guidance throughout my undergraduate and graduate studies. I am deeply privileged to have completed this thesis under his supervision. This thesis would have never been realized without his direct support and assistance.

I would also like to take this opportunity to thank my parents for allocating their time and effort to grant me the chance of becoming all I could and wanted in life. It would take more than a lifetime to make up for all the sacrifices you made to me.

TABLE OF CONTENTS

LIST OF FIGURES

Description **Page**

LIST OF TABLES

Description **Page**

LIST OF SYMBOLS

Symbols		Represents
α	=	Lumped constant of proportionality
α_c	=	Diameter correction factor
β	=	Proportionality coefficient
χ	=	Ratio of stiffness of existing foundation to underpinned foundation
δ	=	Effective stress angle of friction for the soil-shaft interface
ϕ	=	Angle of shearing resistance of soil.
ϕ'	=	Effective angle of shearing resistance of the soil
γ	=	Unit weight of the soil
γ_{sat}	=	Saturated unit weight of the soil
γ_{unstat}	=	Unit weight of unsaturated soil
λ	=	Proportion of load carried by underpinning piles
ν	=	Poisson's ratio
σ'_{vz}	=	Vertical effective stress
τ	=	Maximum shear stress
A_c	=	Area of pile grout
A_p	=	Area of pile tip
A_y	=	Area of steel reinforcement

c	=	Cohesion of the soil
C_1, C_2	=	Subsoil parameters
CPT	=	Cone Penetration Test
c_u	=	Undrained cohesion
D	=	Expanded pile diameter
D	=	Effective pile diameter
E	=	Young's modulus of the soil
E_{def}	=	Deformation modulus of subsoil
E_p	=	Young's modulus of the pile
E_s	=	Modulus of horizontal subgrade reaction
f'_c	=	unconfined compressive strength of the grout
f_s	=	Ultimate unit skin friction of the soil
f_{si}	=	Ultimate unit skin friction for the soil layer i
f_y	=	Characteristic yield stress of reinforced steel
H_1	=	Thickness of upper soil layer
H_2	=	Thickness of lower soil layer
I_L	=	Non-dimensional coefficient of form
I_P	=	Moment of inertia of the pile
K	=	Coefficient of earth pressure
K_o	=	Coefficent of lateral earth pressure at rest
K_1, K_2	=	Values of the modified Bessel functions

L = Length of Pile

L_{st} = Slope tangent value of load from load-displacement graph

L_2 = Interpreted failure load

m = Number of soil layers

N = Number of blow from SPT test

N_c^* = Bearing Capacity factor

n_e = Integer number to yield minimum critical buckling load

n_{found} = Factor of safety of foundation

n_{pile} = Factor of safety of pile

OCR = Over Consolidation Ratio

P = Applied Load

p_1 = Limit pressure from pressuremeter test

p_1^* = Modified limit pressure

P_{cr} = Critical load

P_g = Grout pressure

P_p = Pile load taken by underpinning piles

P_{tot} = Total applied load on foundation

Q = Load Carrying Capacity

$Q_{allowable}$ = Allowable Carrying Capacity

q_c = CPT resistance

Q_{fl} = Critical buckling load

Q_i = Load capacity load

Q_p = End-Bearing Capacity

q_s = Limit unit shaft resistance

$q_{s\ max}$ = SPT resistance

Q_s = Ultimate skin friction Capacity

$Q_{s(allowable)}$ = Allowable Skin Friction Capacity

$Q_{s(L1)}$ = Interpreted skin friction capacity using L_{st} method

$Q_{s(L2)}$ = Interpreted skin friction capacity using L_2 method

Q_w = Design ultimate axial load

s = Steel partial factor

S_F = Foundation displacement

SPT = Standard Penetration Test

S_{ti} = Total settlement of foundation at time t_i

s_u = Undrained shear strength

t = Time

u = Pore water pressure

z = Depth

CHAPTER 1

INTRODUCTION

1.1 OVERVIEW

In 1952, an Italian contracting company began designing piles with diameters smaller than anticipated by several construction codes of that time. These piles were first introduced as *Pali radice* (Bruce, 1994). Two decades later, the technique was brought to North America by the same company, where micropiles were used for several underpinning jobs in the city of New England, Massachusetts. The technique was viewed with **s**kepticism in the U.S for years and its rapid growth did not begin until 1987. Today, micropiles are widely used for underpinning elements to arrest settling existing structures, as a form of enhancement to bearing capacity, and to support existing foundations when excavations are proceeding adjacent or right below them. Micropiles have been also applied for in situ soil reinforcement projects needed to strengthen the underlying soils and to stabilize slopes and landslides. They have gained enormous popularity in the deep foundations domain, knowing they can be drilled through difficult subsoil conditions, and cause minimal disturbance to the existing structure and its surroundings (Bruce et al, 1999). In addition, micropiles have also the advantage of being drilled under difficult conditions with equipments operating at low headroom and confined spaces.

In spite of all the benefits micropiles bring for foundation support and in situ soil reinforcement, their applications are scarcely applied in North America. Further research is consequently needed in order to enhance their use. Most of the studies conducted on drilled shafts and micropiles in particular were based on analytical and field results in sand and clay where the soil-pile interface

is relatively smooth. In consequence, design equations under these conditions may not fully adhere to micropiles embedded in gravelly soils where the roughness of the soil-shaft interface and the impact of dilatancy can both increase the bearing capacity. A detailed study on micropiles embedded in gravelly soils is therefore needed.

The purpose of this report will be to examine some important aspects in the theory of micropiles, and provide design procedures that quantify and classify the skin friction of micropile foundations embedded in gravelly soils.

1.2 THESIS OBJECTIVES

The major components of this report will be:

a) To provide a literature review on micropiles and their applications.
b) To carefully examine the design procedures of micropiles in granular soils.
c) To develop a numerical model capable of measuring the skin friction of micropiles embedded in gravelly soils.
d) To validate the numerical model with existing field test results.
e) To generate data from the numerical model in order to evaluate the skin friction of micropiles embedded in gravelly soils.
f) To conduct a parametric study on the capacity of micropiles embedded in gravelly soils.
g) To develop a design approach for skin friction of micropiles embedded in gravelly soils.
h) To present conclusions on skin friction of micropiles embedded in gravelly soils based on the findings of this present report.

CHAPTER 2

LITERATURE REVIEW

2.1 PILE FOUNDATION OVERVIEW

Piles consist of long, slender pre-fabricated or cast-in-place structural members that are constructed to support new structures. They are mainly used when the bearing strata are found at great depths below the ground level and/or the structural loads are so high that spread footings would not withstand. Piles can also be adapted to support existing foundations undergoing significant settlements or suspected to fail, a technique often referred to as underpinning.

Piles are available from a wide range of types, all falling within the categories of displacement or non displacement types (Thoburn and Hutchison, 1985).

Displacement piles are forced or driven into the ground by vibratory or hammering methods, whereas non displacement piles are formed or placed in a hole excavated by augering methods, a technique also referred to as drilled shafts (Coduto, 2001).

The material used for pile foundation generally consists of steel and pre-cast concrete for displacement piles, or grout (sand-cement water mix) reinforced with steel for non-displacement piles. The shapes and materials of piles are generally dictated depending on the requirements of each project.

Piles are designed to withstand axial loads which are either compressive or tensile, and lateral loads. When compressive loads are applied, conventional piles resist the loads using both side

friction and toe bearing resistance (Coduto, 2001). Tensile loads, generally occurring from uplift pressure of the soil, are resisted by the skin friction and the weight of the pile itself. Lateral loads exert shear and moment on a pile, which are resisted by the stiffness of the pile and its surrounding soil. Figure 2.1 illustrates the transfer of structural loads from a conventional pile into the surrounding soil:

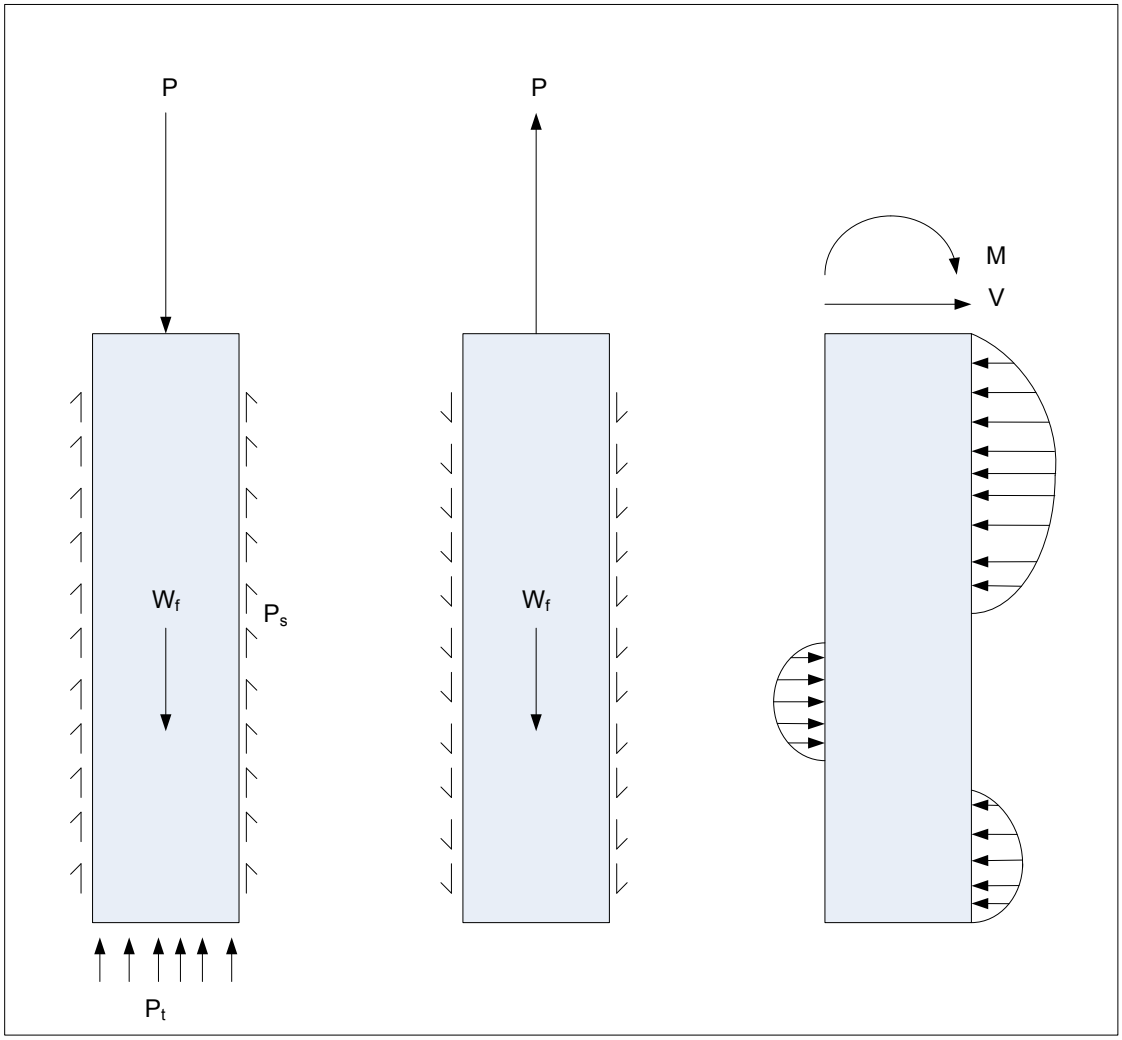

Figure 2.1. Transfer of structural loads from a conventional pile to the surrounding ground: Compressive loads, axial tensile loads, lateral loads.

2.2 LITERATURE REVIEW OF MICROPILES

Bruce et al. (1999) defined a micropile as a small-diameter (less than 300mm) non displacement pile composed of placed or injected grout, and having some form of steel reinforcement to resist high proportions of the design load. The load exerted on the micropile is essentially absorbed by the steel, which occupies up to 50% of the entire micropile volume, and transferred through the injected grout to the surrounding rock or soil mass. The steel reinforcement is the major element carrying the load, and the grout serves to transfer the latter, by friction, to the surrounding soil. End bearing contribution is minimal in micropiles, given the nominal geometries involved. The grout/ground strength is achieved majorly by the subsoil conditions and the grouting method used (Armour and Groneck, 1998). The drilling technique could also play a significant role, yet less well quantified. Figure 2.2 illustrates the typical construction sequence of a single micropile.

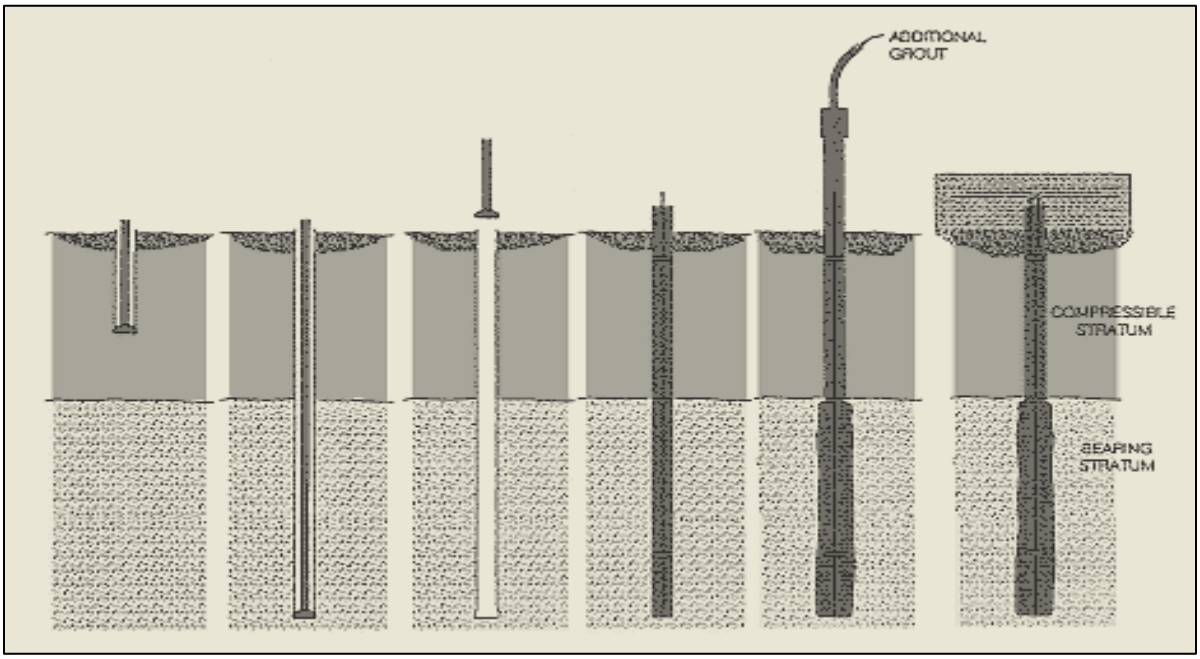

Figure 2.2. Typical construction sequence of a single micropile (Armour and Groneck, 1998).

Micropiles range between 100 and 250 mm in diameter, 20 to 30 m in length, and 300 to 1000 kN in compressive or tensile loads, although compressive loads of over 5000 kN have been recorded (Bruce et al., 1999).

Other technical terms have been used to define micropiles, including pinpiles, minipiles, needle piles, pali radice and root piles. However, these terms all refer to the "special type of small diameter bored pile" as described by Koreck (1978).

Micropiles provide practical solutions for structural support and for In situ soil reinforcement (Armour and Groneck, 1998). Their applications are mainly used in the following domains:

a) Underpinning of existing foundations.
b) Foundation for new structures.
c) Enhancement of bearing capacity for existing structures.
d) Settlement reduction.
e) Soil strengthening and landslide stabilization.
f) Structural stability.

Micropiles can be favored over other piles, because they can be drilled under difficult subsoil conditions and the drilling equipments can function under limited overhead clearance. In addition, they allow minimum settlements to the existing and surrounding structures, and they provide high unit loads ranging from 300 kN to 5000 kN.

In 1997, The Federal Highway Administration (FHWA) of the United States of America provided a comprehensive literature review on micropiles that included laboratory and field testing data, design methods, construction methodologies, site observations and monitored case studies. The report, entitled *Drilled and Grouted Micropiles, State-of-the-Practice Review*

(Bruce and Juran, 1998), contains a unique and innovative classification system for micropiles based on two main criteria:

a) Philosophy of behavior (design)
b) Method of grouting (construction)

The philosophy of behavior establishes the method used in designing the micropile, while the method of grouting dictates the grout/ground bond capacity, which is generally the major constructional element for pile capacity. The same report discussed a classification system that contains a two-part designation: a number that denotes the type of design that shall be used, and a letter assigned to the method of grouting.

According to Bruce and Juran (1997a), the philosophy of behavior can be classified in two principle cases:

1. Case 1: directly loaded piles (individual or group of piles), whether for axial or lateral loading conditions. The pile reinforcement in this case resists most of the applied load.
2. Case 2: 'root piles', with support and stabilization by locking onto a three dimensional network of reticulated piles forming a soil/pile composite structure. The latter is referred to as a reticulated pile network.

Case 1 micropiles can be used as alternatives to transfer the structural loads to a deeper and stronger soil layer. In this case, the applied load is primarily resisted by the steel reinforcement and transferred to the soil through the injected grout.

Case 2 micropiles, also known as a reticulated pile network, are mainly used for stabilization and support. In this case, the structural support is resisted by the entire reinforced soil mass.

The method of grouting directly affects the grout/ground bond capacity. The classification in this case consists of a letter designation (A through D), based on the following criteria:

a) Type A: grout is placed in the pile under gravity head only. Sand cement mortars, as well as neat cement grouts, can be used because the grout column is not pressurized.
b) Type B: neat cement grout is injected into the drilled hole as the temporary steel drill casing is withdrawn. Pressures are typically in the range of 0.3 to 1 MPa.
c) Type C: neat cement grout is placed in the hole, as done for type A. After 15 to 25 minutes, before hardening of this primary grout, similar grout is injected once via a preplaced sleeved grout pipe at a pressure of at least 1 MPa. This type of pile is common practice only in France.
d) Type D: neat cement grout is place in the hole, as done for Type A. Some hours later, when this primary grout is hardened, similar grout in injected via a preplaced sleeved Grout pipe. In this case, however, a packer is used inside the sleeved pipes so that specific horizons can be treated several times if necessary, at pressures of 2 to 8 MPa.

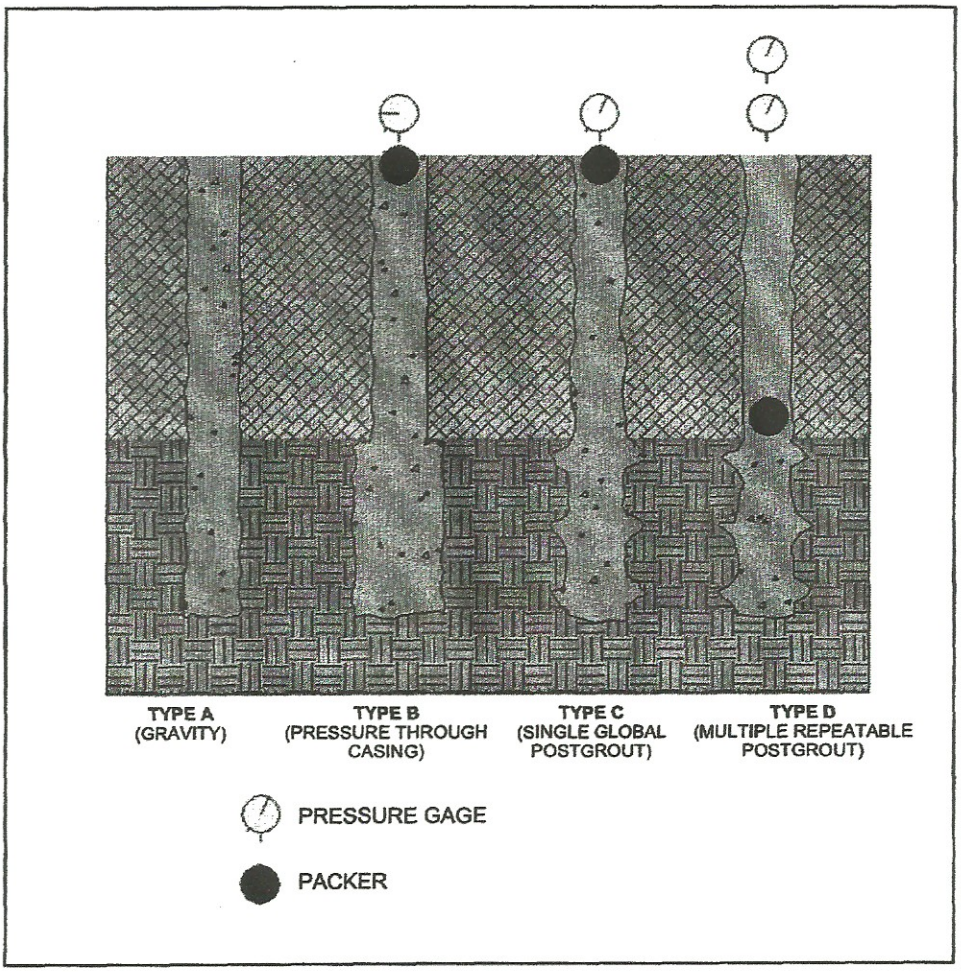

Figure 2.3. Classification of a micropile based on the method of grouting (Armour and Groneck, 1998).

Armour and Groneck (1998) stated prominent factors that influence the type of micropiles to be chosen:

a) Physical Considerations:

Micropile drilling equipments have the advantage of being installed in restricted areas with low headroom and confined space. Unlike conventional piles, micropiles can be installed

within a few millimeters of existing walls or foundations and the equipments can be mobilized in up steep slopes and remote locations.

b) Subsoil Conditions:

Micropiles have the benefit of being installed through difficult subsoil conditions, ranging from cobbles and boulders to loose granular soils and soft clays. In addition, high groundwater conditions cause minimal disturbance to micropile installations and are an especially favorite option where there are subsurface voids caused by karstic limestone.

c) Environmental Conditions:

Because of their parametric configurations, micropiles cause less spoil from drilling than other conventional pile systems. The grout mix can be designed to withstand chemically aggressive ground water and soils. Installation of micropiles causes less disturbance and noise then conventional piling techniques, thus minimizing disturbance of adjacent foundations. The latter is a major benefit for projects conducted in congest urban areas.

2.3 THE USE OF MICROPILES IN UNDERPINNING

Bullivant and Bradbury (1996) acknowledged that settlement problems have occurred with us since the earliest times. Science was then limited in the design of foundations, and any knowledge regarding the existing soils and structures was acquired from local experience and the skills handed down by the artisans. It wasn't till the seventeenth century that a scientific approach was actually applicable, when lime came into use as the matrix for mortars and concretes made it more practicable to improve defective foundations. Almost exclusively, the

work involved techniques that can be grouped under the heading 'traditional underpinning' (Bullivant and Bradbury, 1996). This technique involves the casting of mass concrete beneath the existing foundation and hence transferring the load to deeper and more competent strata. The method involves excavation of the soil beneath the existing foundation to a depth typically not exceeding 1.5m, and filling the void created with concrete. The traditional approach is widely used today, yet it has drawbacks and relies often on the arbitrary approval of an excavated base beneath the existing foundation, usually conducted without an adequate soil investigation, thus making it a risky process.

The introduction of pile foundation has brought an innovative perspective in geotechnical engineering. The latter enabled foundations to reach more competent strata and gave the opportunity to design foundation on the basis of the load bearing capacity of a single pile which could be verified by direct load test (Lizzi, 1982). However, conventional piles are quite troublesome when used for underpinning elements. Driven piles generally cause major disturbance to nearby structures and are therefore disregarded. Cast-in-situ piles (vertical, minimum diameter 400mm) are sometimes applied for underpinning. The shafts are casted right next to the walls and then connected the structure by reinforced concrete beams. This method involved the some cutting of the nearby walls, which is troublesome and dangerous during the construction period.

The introduction of 'palo radice' (root piles) in 1952 by the Italian firm Fendedile of Naples marked a major milestone in the restoration of old structures. The latter is constructed in the same fashion as a single micropile, shown earlier in figure 2.2 of this report.

Lizzi (1982) wrote that micropiles are ideal underpinning elements for the following reasons:

a) Their execution did not introduce, even temporarily, any undue weakness or overstress in the structure as well as the soil.
b) They responded immediately to additional structural movement.
c) 'pali radice' can be drilled under difficult subsoil conditions, including boulders, old foundations or other obstructions it may contain.
d) They enabled the assessment of a new factor of safety (n), which will be $n = n_{found} + n_{pile.}$

Lizzi (1982) elaborates that a 'pali radice' used in underpinning is not completely utilized, compared to its full capacity: it could always bear much more than the assigned load, but it would lead to unwanted settlement in the existing foundation. He introduced, as shown in the advantages mentioned earlier, a new factor of safety for foundations underpinned with 'pali radice':

$n = nf + np$

Where:

$nf > 1$ factor of safety for the existing foundation

$np = P_{ult}/P_{all}$ factor of safety for the additional piles (P_{ult} = ultimate load, P_{all} = allowable load).

In the early stages, the factor of safety consists of both the safety of the existing foundation and that of the pali radice. The latter is due to the fact that pali radice function is complimentary and will only contribute when necessary; Once the structure undergoes settlement, the piling responds immediately and takes part of the total load, thus reducing the stress imposed on the

subsoil. Subsequent settlement would impose more loads on the piles until, eventually, the entire foundation is fully supported by them, and thus nf becomes negligible.

Bruce and Juran (1997a) acknowledged that micropiles are widely used as underpinning elements, mainly to enhance bearing capacity and reduce settlements of existing foundations. Other purposes may include:

a) Arresting and preventing structural movement.
b) Repairing/replacing deteriorating or inadequate foundations.
c) Adding scour protection to their original elevation.
d) Transferring loads to deeper strata.

Tsukada et al. (2006) provided an extensive investigation on the enhancement of the bearing capacity of existing footings reinforced with micropiles. The aim of the study was to examine some important aspects which classify and quantify the development of bearing capacity in micropiles foundations. Model tests were thus performed with and without micropiles reinforcement on different layers of sandy soils which are loose, medium dense and dense. Three types of micropiles with different bending stiffness and surface roughness were used. The model tests consisted of circular footings that were reinforced with a group of micropiles and the arrangement of the micropiles was varied as well as the inclination of the micropiles. In the model tests, parametric variations of the number, length, and the inclination of the micropiles were adopted.

Figure 2.4 illustrates the series of loading tests that were conducted in the investigation. The first test, denoted by the authors as F-T shown by figure 2.4 (a), was conducted to observe the load-

displacement behavior of the circular footing without any reinforced micropiles. The second series of tests, denoted as MP, were conducted on a circular footing model suspended from the ground and reinforced with a series of micropiles, as shown Figure 2.4 (b). The type, length, number and skin roughness of micropiles were modified in this series. The third series of tests, denoted as FT-MP were conducted on circular footing models reinforced with vertical or inclined micropiles. Similar to the second series, the length, number, and skin roughness were modified in each test.

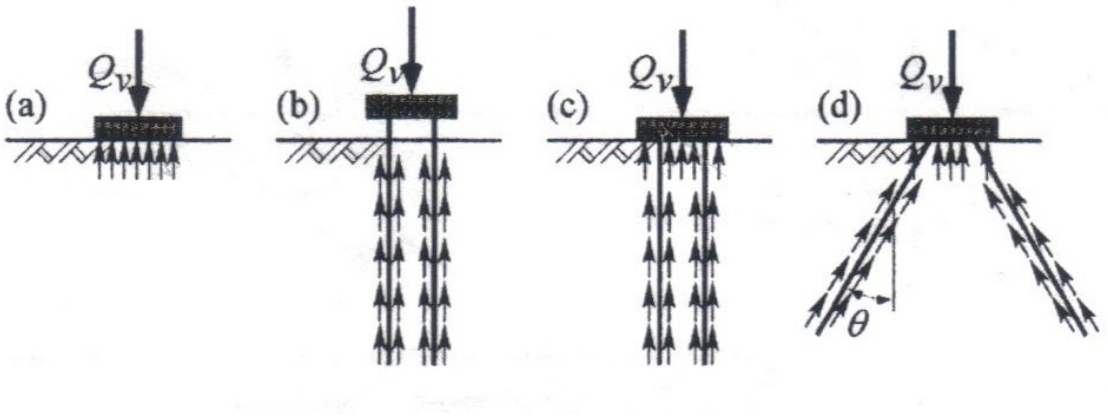

Figure 2.4. Schemes of the loading tests: (a) FT-Tests, (b) MP – Tests, (c) MP FT-Tests with vertical micropiles and (d) MP-FT-Test with inclined micropiles (Tsukada et al., 2006).

The FT- tests results were compatible with the existing theoretical models. In the case of the dense sand, the behavior was of the general shear type. Failure was thus noticed on the surface plane. For medium and loose sand, the behavior was of the local shear type. Failure in these cases did not appear on the surface plane. The differences in the shear failure and loading behavior would be attributed to the dilative properties of sand as a function of the relative density.

The MP- tests revealed that the bearing capacity of the medium and loose sand happens to be less than half than that of the dense sand. This remarkable difference in bearing capacity with the reduced relative density can be attributed to several factors, including the reduction in the angle of internal friction, and the reduced values in the confining stress around the micropiles as induced by the contractive nature of medium and loose sand. The influence of surface roughness was also remarked. The tests revealed a 50% improvement in the bearing capacity due to the improvement of the fixity of micropiles within the sand, as well as a slight increase in the diameter. The group effect of micropile, which is followed by the reduction in the bearing capacity per pile with increasing number of piles, was not recognized.

For MP-FT tests, the dilative properties of sand played an important factor on the type of shear and displacement behavior. In dense sands, the horizontal displacement of the sand would be confined within a group of micropiles in the loading process, and the confinement would modify the end bearing and the skin friction of the micropiles. Hence, if the sand is dense and dilative, the confining pressure would increase more, otherwise it would decrease. The tests revealed that the bearing capacity of micropile groups in loose and medium dense sands is less than half of that in dense sand. It remains to be seen whether such conclusions can be made with gravelly soils.

This study proved existing theoretical facts; an increase in the confining pressure on the surface of micropiles due to the dilatant behavior of dense sand would raise remarkably the skin friction of micropiles. An increase in the relative density brought about an increase in the ultimate unit skin friction f_s for micropiles. The study also concluded that the ultimate unit skin friction f_s and bending stiffness of micropiles are essential in increasing the bearing capacity of micropiles.

2.4 REVIEW OF CURRENT DESIGN PROCEDURES FOR MICROPILES

The design of micropiles differs little from that required for any type of conventional piles: the system must be capable of sustaining the anticipated loading requirements within acceptable settlement limits, and in such fashion that the elements of that system are operating at safe stress levels.

Although conventional piles are usually governed by external carrying capacity, Bruce (1994) stated that micropiles are majorly controlled by the internal designs, which are the pile components. That latter reflects both the relatively small cross section available and the unusually high grout/ground bond capacities that can be mobilized, as a consequence of the micropile installation methods.

According to Dringenberg and Craizer (1990), there are three essential causes for the failure of a pile:

1. Failure of the ground (External Design)
2. Buckling of the pile.
3. Internal failure of the pile.

Mascardi (1982) added that the ultimate load that can be supported by a single micropile is defined by three lowest of the causes mentioned above.

Bruce and Juran (1997b) have later classified the general design of micropiles into two major categories:

a) Evaluation of the structural (or internal) resistance of the (composite) micropile section that is governed by its area and the strength of the reinforcement provided.

b) Geotechnical (or external) evaluation of the ultimate capacity of the micropile, which requires appropriate determination of the grout/ground bond interface parameters and the initial state of stress in the ground after micropile installation.

This thesis is intended to focus on the geotechnical features of micropiles embedded in gravelly soils. Yet, a brief section is allocated to the internal design of micropiles.

2.4.1 Internal Design of Micropiles

The two major components for the internal design of a micropile are steel reinforcement and grout. Several factors dictate the nature of the reinforcement used, including the scope of the project, the required working load and permissible elastic deflection. Grout, which consists of water and cement, is measured by the water to cement ratio (w/c). The latter usually fluctuates from one case to another, depending on the nature of the groundwater or by the strength/time requirements (Bruce, 1994).

Lizzi (1982) argued that relatively small-capacity Pin Piles designed to act only in compression usually comprise either a cage of high yield reinforcement bars supported by helical reinforcement, or a very limited number of high-strength bars. When such piles have to act in

tension, the latter solution is adopted. Thus, the internal design of a micropile would differ depending on whether it's subjected to compression loads or tensile loads.

The design in compression for a micropile is numerically calculated using the following equation (Bruce and Juran, 1997b):

$$Q_w = g \times f'_c \times A_c + s \times f_y. \times A_y$$

For tension micropiles, the equation is:

$$Q_w = s' \times f_y \times A_y$$

Where

Q_w = Design ultimate axial load.

f'_c = Characteristic unconfined compressive strength of the grout.

A_c = Area of pile grout.

f_y = Characteristic yield stress of reinforcing steel.

A_y = Area of steel reinforcement.

g,s, and s' = Partial factors for the materials that ensure that the mobilized stress levels in the steel and grout are limited to acceptable values (values specified by the design codes).

Table 2.1 summarizes the allowable design stresses in steel and grout cement in accordance to American design codes, including AASHTO (1992), MBC (1988), and BCNYC (1992).

Table 2.1. Allowable stress level in steel and grout cement in accordance to BCNYC (1991), AASHTO (1992) and MBC (1988).

Codes	BCNYC	AASHTO	MBC
Casing/pipe	0.35 f_y	0.25 f_y	0.4 f_y
Grout cement	0.25 f'_c	0.40 f'_c	0.33 f'_c
Core/Rebar	0.5 f_y	0.25 f_y *	0.4 f_y

* with casing, without casing: Rebar = 0.2975 f_y and grout = 0.253 f'_c

The allowable working load is conducted by dividing the ultimate axial load by an appropriate factor of safety. According to AASHTO (1992), a factor of safety of 1.5 is normally adopted.

Gouvenot (1975) and Mascardi (1982) both concluded that failure of micropiles through buckling may only take place in soils with deplorable mechanical properties such as loose silts, plastic clay or peat.

In general, buckling of piles depends on the soil-pile interaction, which involves the pile section and elastic properties, soil strength and stiffness as well as the eccentricity of the applied load. Buckling is generally not the decisive factor for the micropile design (Bruce, 1994).

2.4.2 External Design of Micropiles

The load transfer mechanism of micropiles depend on several parameters, including the installation technique; drilling and grouting pressure; initial state of stresses; engineering

properties of the underlying soils (relative density, permeability, and shear strength properties) (Bruce and Juran, 1997b).

Hanna and Nguyen (2003) stated that the load transfer from the micropile to the adjacent ground requires some relative movement. The latter is controlled by the elastic modulus of the composite-reinforced micropile and the load transfer mechanism.

Some micropiles are fully bonded along their entire lengths, while other micropiles are partially bonded where casing is kept through the upper soft layers to prevent negative skin friction.

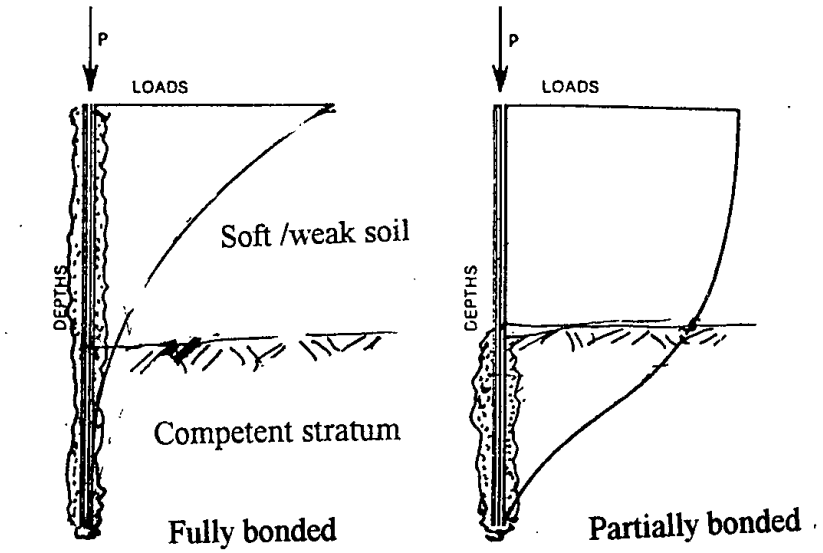

Figure 2.5. Typical load-transfer curves from a "partially bonded" and a "fully bonded" micropile to the soil (Lizzi, 1982).

Micropiles can be subjected to both tensile and compressive loading. Generally, the shape of the load displacement curves obtained from axial compression and tension tests are similar, although

movements are larger in tension. Therefore, most of the existing methods for analyzing compression tests can also be applicable to tensile results (Hirany and Kulhawy, 1989).

When compressive axial loads are applied on a micropile, the load carrying capacity Q is ideally transferred to the soil by both the ultimate skin friction capacity Q_s and the end-bearing capacity Q_p of the pile. Thus, the total load is equal to

$$Q = Q_p + Q_s \qquad (1) \qquad \text{(Bruce and Juran, 1997b)}$$

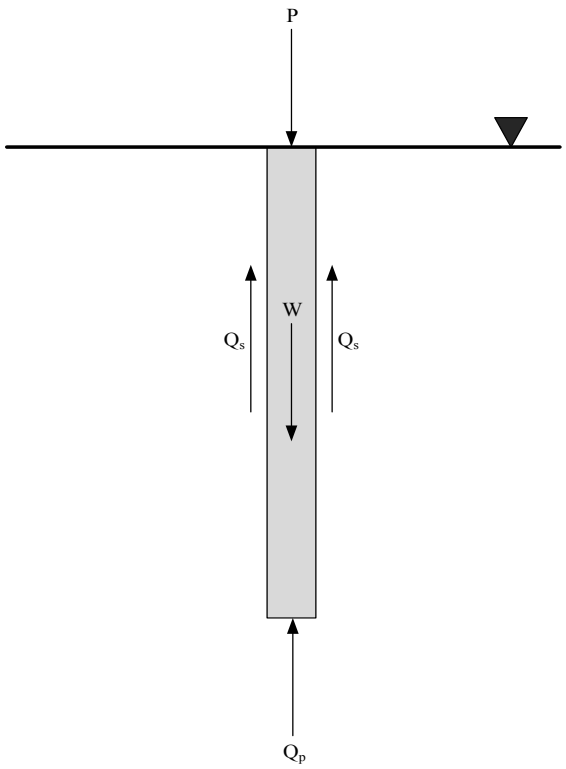

Figure 2.6. Load-transfer behavior of a drilled shaft subjected to an axial compressive load.

However, the geotechnical design of micropiles is conducted in a fashion where the load transfer to the ground occurs mainly through the grout-to-ground skin friction, neglecting any contribution from end bearing (Bruce, 1994; Bruce and Juran, 1997b). The latter is due to the following reasons:

a) The high grout-to-ground bond capacities that can be attained as a consequence of the micropile installation methods.

b) The area available for the skin friction is significantly greater than that for end bearing. For a pile that is 200 mm in diameter with 6 m long bonded length, the area available for skin friction is 120 times greater than that available for end bearing.

c) The pile movement needed to mobilize frictional resistance is significantly less than that needed to mobilize end bearing. Brown et al (2010) acknowledged that maximum frictional resistance occurs at a relatively small displacement and is independent of the shaft's diameter, while end bearing resistance occurs at a relatively large displacement and is a function of shaft diameter and geometry type.

Bruce et al. (1999) stated that end bearing would only be realistic for moderately loaded micropiles founded on competent rock. Therefore, the end-bearing load Q_p becomes negligible from equation (1).

Jeon and Kulhaway (2002) acknowledged that micropiles have a high ratio of the circumference to the cross-section area, and therefore rely essentially on skin resistance for the load transfer. They added that tip resistance is negligible in most cases.

Lizzi (1985) provided the following empirical formula to quantify the ultimate skin friction capacity Q_s of a micropile:

$Q_s = \pi \times D \times L \times K_1 \times I$

Where

D = Drilling Diameter of Pile.

L = Length of the Pile.

K_1 = Coefficient representing average bond between pile and soil.

I = Non-Dimensional coefficient of form.

The ultimate skin friction capacity Q_s was then developed by the following equation:

$Q_s = \pi \times D \times \Sigma f_{si}\, dl_i$ (2) (AASHTO, 1992)

Where:

f_{si} = Ultimate unit skin friction for the soil layer i.

D = Effective diameter of the micropile.

m = Number of soil layers.

dli = Depth of considered layer.

The ultimate skin friction capacity Q_s is a product of the ultimate unit skin friction f_s and the cylindrical surface area over which skin friction develops at the micropile interface (Brown et al., 2010).

The ultimate unit skin friction f_s varies upon several factors, including the installation method, drilling and grouting pressure, loading type (tension and compression), initial state of stresses, engineering properties of the soil and its relative density (Bruce and Juran, 1997b). The grain size and porosity of the soil in place govern the grout penetrability through the surrounding soils. In granular soils (gravel, sand) and weathered rock, with relative high permeability, grout will penetrate through the surrounding pores. In fine grained cohesionless soils, penetration of the grout through the pores would be problematic; thus increasing the grout pressure would provide a higher radius of grout permeation into the ground and a more effective densification of the surrounding ground. The latter would enhance the grout/ground interface properties and increase the micropile's axial capacity.

The computation of the ultimate unit skin friction f_s is often computed depending on the micropile type (A, B, C or D) and the ground type (cohesionless soils and cohesive soils, soils and rock).

For type A micropiles, the ultimate unit skin friction f_s in cohesionless soils is calculated using the beta β method (Bruce and Juran, 1997b):

$$f_s = \beta \, \sigma'_{vz} \qquad (3)$$

Where σ'_{vz} is the vertical effective stress at depth z and β is the proportionality coefficient.

There are several factors affecting the coefficient of proportionality β, such as local variations to the earth pressure from one site to another, soil characteristics (effective pore size, initial angle of shearing resistance, and soil compressibility) as well as the construction techniques.

Reese and O'Neill (1988) provided an empirical method to measure the coefficient of proportionality β based on a series of 41 drilled shaft load tests. The ultimate unit skin friction in sand was computed by

$$f_s = \beta \, \sigma'_{vz} < 200\text{kPa limit} \qquad (4)$$

Where:

$\beta = 1.5 - 0.245 \, z^{0.5}$ with limits of $1.2 > \beta > 0.25$

The parameter β depends only on the depth and is totally independent of the soil density, although the vertical effective stress found in equation 4 is a function of density.

With subsequent testing, Hassan and O'Neill (1994) provided an empirical relationship correlating β values with the SPT count N. The relation was provided by the following equation

For N > 15 $\quad \beta_{nominal} = 1.5 - 0.42[z(m)]^{0.34}$, $1.2 > \beta > 0.25 \qquad (5)$

For N < 15 $\quad \beta = \beta_{nominal} \; N/15$

The Kulhawy method (1991) to determine the ultimate unit skin friction f_s is based on soil mechanics principles. As illustrated in Figure 2.7, the ultimate unit skin friction f_s is directly proportional to the normal stress acting on the soil-shaft interface.

The ultimate unit skin friction f_s for the Kulhawy method is given by equation (3) and the coefficient of proportionality β is given by the equation

$$\beta = K \times \tan \delta \qquad (6)$$

Where:

K = coefficient of earth pressure at the wall of the drilled shaft at side shear failure.

δ = effective stress angle of friction for the soil-shaft interface.

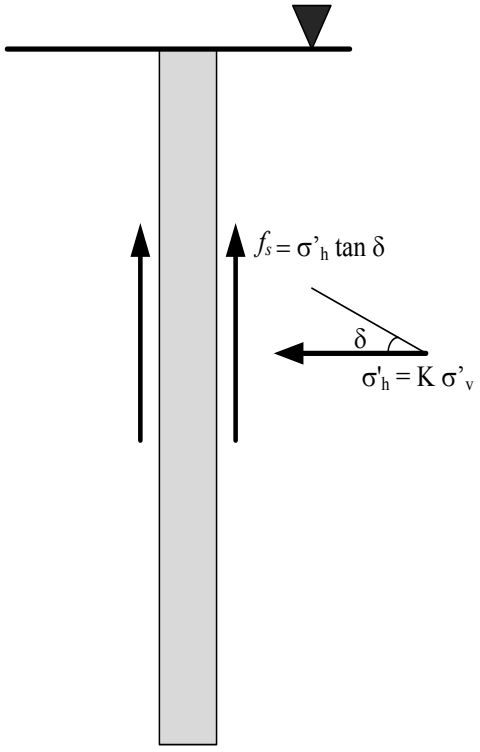

Figure 2.7. Model of unit skin friction for drilled shafts in cohesionless soils (Brown et al, 2010).

Kulhawy (1991) proposed that δ can be expressed as a fraction of the angle of shearing resistance of soil ϕ. A sound construction technique with a rough interface alongside the shaft, the fraction becomes equal to 1. For calculations in this thesis, the fraction δ/ϕ is assumed to be 1.0.The coefficient of lateral earth Pressure K is a difficult parameter to determine. Lateral Earth Pressure K is a function of the original at rest earth pressure K_0, and the stress changes caused by the construction, loading and desiccation. Field tests have shown K values ranging from 0.1 to over 5. A simple relationship to compute K_0 based on the angle of shearing resistance of soil ϕ and the overconsolidation ratio (OCR) is provided by Mayne and Kulhawy's (1982):

$$K_0 = (1- \sin\phi)\ OCR^{\sin\phi}$$

Where OCR refers to the over-consolidation ratio.

The typical values for the angle of shearing resistance and OCR, depending on the type of soil are provided in the following table:

Table 2.2. Typical values for angle of shearing resistance of Soil and Overconsolidation Ratio (Jeon and Kulhawy, 2002).

Soil Type	**ϕ (deg)**	**OCR**
Loose Sand	28-32	1-3
Medium Dense Sand	32-38	3-10
Dense Sand, Gravel	38-45	10-20

By investigating hundreds of load tests, Kulhawy found that K/K_o varies between 0.67 and 1. The main factor affecting this ratio would be the construction method and its influence on the in situ stress.

Hanna and Al-Romhein (2008) conducted an experimental investigation on the at-rest pressure of overconsolidated cohesionless soil acting on retaining walls. The tests results compared well with Kulhawy's empirical formula. The authors further proposed the following empirical formula:

$$K_0 = (1- \sin\phi)\, OCR^{(\sin\phi - 0.18)}$$

Rollins et al. (2005) collected and studied the results of 28 axial tension (uplift) load tests that were performed on drilled shafts in soil profiles ranging from uniform medium sand through well-graded sandy gravel. The purpose of the study was to evaluate skin friction of drilled shafts in gravelly soils. Typical load displacement curves were developed to assess the skin friction. Based on measured skin friction and the angle of shearing resistance, the coefficient of lateral earth pressure K were computed for the load tests. The back-calculated K values were plotted versus depth and the best-fit equation for K was found to be

$$K = 4.62e^{(-0.137z)} \qquad (7)$$

Where z signifies the depth below the ground surface.

Using this empirical relationship, the ultimate unit skin friction f_s was then computed using equation (6) and (3). The computed and measured ultimate unit skin friction f_s values from the

field tests are plotted in figure 2.8 and there's a significant spread about the line indicating perfect agreement. It is revealed form the graph that the computed capacities are no greater than two times the measured values; hence a factor of safety of 2.0 would be ideal in using this particular method. Rollins et al. modifications to Kulhawy's method (1991) were effective for drilled shafts embedded in gravelly soils.

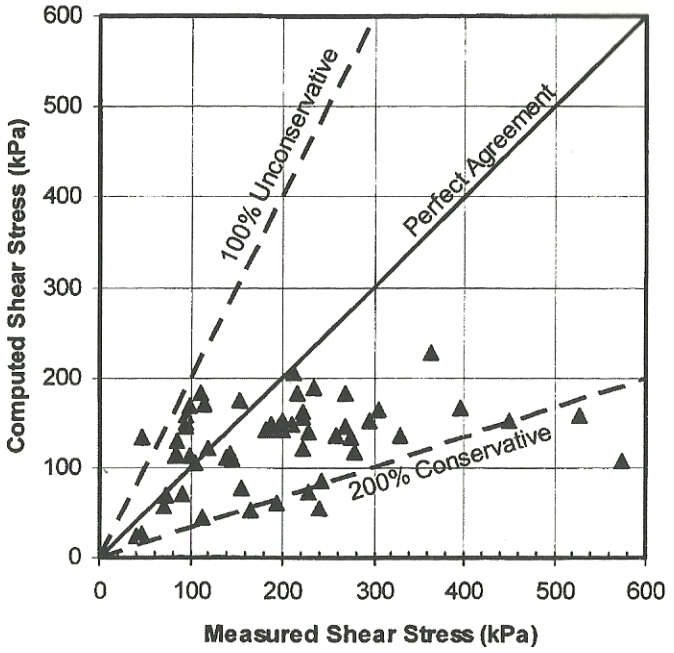

Figure 2.8. Comparison of measured and computed skin friction for load tests in gravel using Kulhawy method (1991) with K estimated in Eq. (7) (Rollins et al., 2005).

Other relationships of β vs. depth have been anticipated by several authors, but no unique relation was developed due to the various factors affecting the coefficient of proportionality β (Bruce and Juran, 1997b).

The ultimate skin friction capacity Q_s for type B micropiles in cohesionless is measured through the following expression:

$$Q_s = \pi \text{ x } D \text{ x } \Sigma f_{si}\, dl_i$$

Where:

f_{si} = Ultimate unit skin friction for the soil layer i.

D = Effective diameter of the micropile.

m = Number of soil layers.

dli = Depth of considered layer.

This is the same expression used to calculate the skin resistance for type A micropiles. Yet, the ultimate unit skin friction f_s is measured using the following equation:

$$f_s = p_g \,.\, \tan Ø'$$

Where:

p_g = Grout pressure.

$Ø'$ = Effective angle of shearing resistance for the soil, usually obtained from empirical Correlations of SPT vs. Ø.

The β method used for type A micropiles has been also used for pressure grouting type B micropiles, given by the following expression:

$$\beta = K_1 K_2 \tan Ø'$$

Where:

K_1 = Earth pressure coefficient.

K_2 = Coefficient representing the increase in effective diameter of the pile shaft due to grouting pressure.

Littlejohn (1970) has recommended values for K_1 that range between 1.4 and 1.7 for compact sand ($Ø^{'} = 35^0$) and compact sandy gravel ($Ø^{'} = 40^0$), with K_2 varying ranging between 1.2 and 1.5 for dense sand, 1.5 and 2 for medium sand, and 3 and 4 for coarse sand and gravels.

Littlejohn (1980) also recommends a combined $K^{'}$ factor (i.e., K_1 x K_2) ranging from 4 to 9, with $K^{'}$= 4 for finer gravel and $K^{'}$= for coarser materials. The latter is only applied for type B micropiles, where grout injection pressures range between 0.3 and 0.6 MPa.

Types C and D micropiles are installed using high pressure grout surpassing 1MPa. The latter is conducted using multiple grouting sessions or innovative grouting techniques. High pressure grout could cause fissure that interlocks with the surrounding ground, thus increasing considerably the axial loading capacity of the micropile. Types C and D micropiles are usually selected when the subsoil conditions are loose and high pressure grouting is needed to create a stronger grout-ground bonding. The scope of this current thesis will be to focus on micropiles type A where the grout is poured through gravity head only.

CHAPTER 3

NUMERICAL MODEL

3.1 GENERAL

In micropiles, skin friction resistance is considered to be the essential element carrying the applied loads. End bearing resistance is negligible given the micropile's parametric configurations. For micropiles embedded in gravelly soils, the grout is generally applied using gravity head only. Hence, type A micropile is generally ideal for design. Grouting with pressure as executed by type B, C and D is not necessary, because there is enough friction between the surrounding soil and the grout to generate adequate resistance with relatively small movement. Multiple grouting is generally needed when the surrounding soil consists of fine sand, silt or clay where pressure is needed to allow grouting to interlock with the surrounding pores.

Current design equations are mostly attributed for sand and clay where the soil-shaft interfaces are much smoother. Such theories may provide conservative results for gravelly soils, where an increase in the capacity can be anticipated because of the roughness of the soil-shaft interface. Figure 3.1 reveals the difference in the soil-shaft interface roughness between sand and gravel.

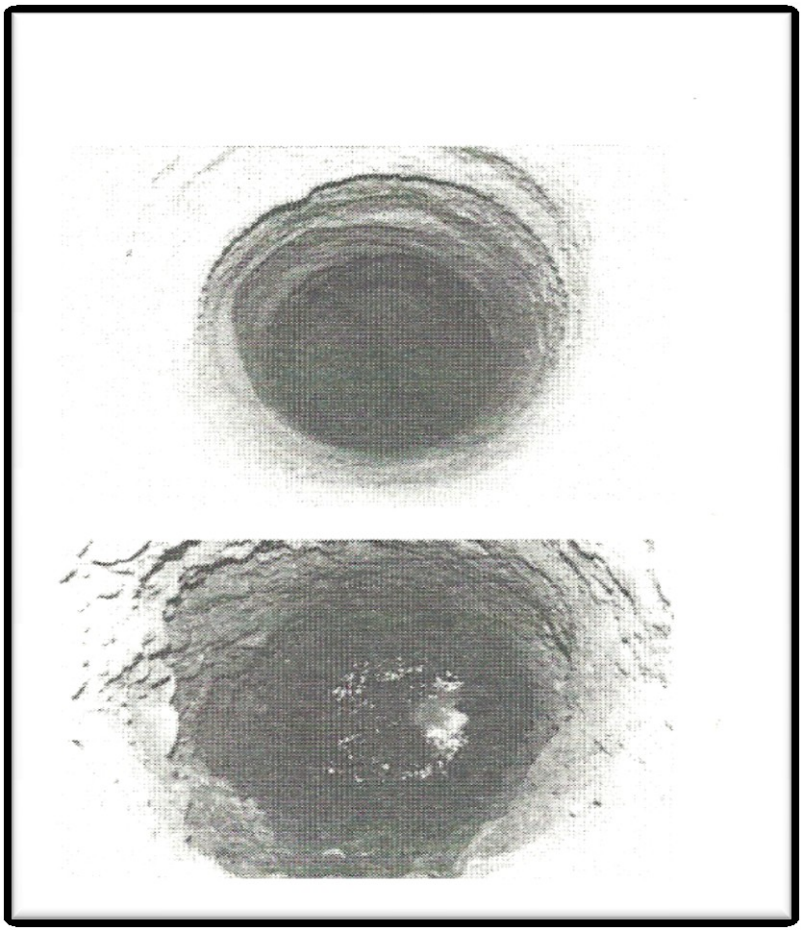

Figure 3.1. Roughness of the soil-shaft interface for Sand (top) and Gravel (bottom)

(Rollins et al., 2005).

This present study investigates the current design equations concerning skin friction for drilled shafts in cohesionless soils, and develops a numerical model capable of generating data that is needed in order to present innovative design procedures for the skin friction of micropiles embedded in gravelly soils.

The study will be conducted on micropiles that abide to the following conditions:

1) Pile/Soil interaction:

   Type 1 micropile, load applied directly under axial loading conditions.

2) Grouting Technique:

   Type A, grout is placed under gravity head only. The micropile is fully bonded with the surrounding soils.

3) The cross-sectional radius will be uniform along the interface, but may vary in dimension from one test to another

3.2 GEO5 SOFTWARE PROGRAM OVERVIEW

Several computer programs currently exist in the civil engineering field that provide the practitioner engineers with adequate solutions needed in their respective professions. These software programs serve a wide variety of civil engineering disciplines, including geotechnical engineering, structural engineering, hydraulic engineering, transportation engineering and environmental engineering. In the geotechnical engineering domain, the software programs allow to solve numerous foundation problems including bearing capacity of strip and raft foundations, ultimate and allowable loads of pile foundations, slope stability, retaining walls, earth retaining structures, embankments, tunnels and underground structures.

GEO5 software program kit allows the user to solve a variety of geotechnical engineering problems that are mentioned above. Each program is used to analyze a different geotechnical task but all modules communicate with one another to form an integrated suite. The program has enjoyed wide success in the geotechnical engineering domain for its user-friendly interfaces and

its versatility to solve a wide range of problems. The programs are based on typical analytical methods and the Finite Element Method (FEM).

3.3 GEO 5 PROGRAM FOR PILES

The software program GEO5 for piles analyzes the limit loading curve, distributions of forces and displacements developed along the pile through the vertical spring method. The program includes a Finite Element Method (FEM) approach, where the pile is represented by standard beam elements, and the response of surrounding soil follows from the solution of layered subsoil as a generalization of the Winkler and Pasternak models. The Winkler model has been used effectively in geotechnical analyses of a beam on an elastic soil layer and pile behaviors resulting from horizontal loads (Tanahashi, 2007). The model originated from Winkler's hypothesis, which states that the deflection at any point on the surface of an elastic continuum is proportional only to the load being applied to the surface and is independent of the load applied to any other points on the surface (Winkler, 1867). This hypothesis leads to a mechanical model of a continuum that is assumed to consist of mutually independent vertical linear springs.

In the Finite Element Method (FEM), the elastic rigid plastic response in shear is assumed along the soil pile interface in view of the Mohr-Coulomb failure criterion. The normal stress acting on the pile is determined from the geostatic stress and soil pressure at rest.

The influence of groundwater is introduced into the shear bearing capacity and the depth of influence zone below the pile heel.

The pile could attain incompressible subsoil, which substantially influences its response. This effect is also taken into account in the program. The pile settlement can also be influenced by the settlement of the surrounding terrain. In particular, settlement of soil may reduce the pile bearing capacity. The pile settlement increases without increasing load. This phenomenon usually exists in cohesive soils and is known as negative skin friction. The latter is not in the scope of this current thesis.

The solution procedure for the bearing capacity of the pile in the Finite Element Method consists of several steps:

1) The pile is represented as a member composed of several beams. The minimum number of beams is 10.
2) Each element is supported at its bottom node by a spring. The spring stiffness serves to model both the shear resistance of skin and the pile heel the stiffness of soil below the pile heel.
3) For each element the limit value of shear force transmitted by skin T_{lim} is determined.
4) The pile is loaded at its top end by increments of the vertical load. For each load increment the magnitude of spring force for each element is determined. This value is then compared with the value of T_{lim} for a given element. If a certain spring force exceeds the value of T_{lim} its magnitude is set to T_{lim}. Analysis for this load increment is then repeated so that the force is redistributed into other springs. Such an iteration within each load increment proceeds as long as each currently active spring does not transmit force that is less than its corresponding T_{lim}. Gradual softening of individual springs results in deviation of the limit loading curve from linear path. It is evident that for a certain load level all springs will no longer be capable of increasing its force and the pile begins to

settle in a linear manner supported only by the heel spring that has no restrictions on the transmitted force.

5) As a result, the analysis provides the limit loading curve, forces developed in the pile and a graph showing variation of shear as a function of deformation at a given location.

For each element of the analyzed pile, the program determines the limiting value of the force that can be transmitted by the pile skin at the location of a given element. Its value depends on the geostatic stress

$\sigma_z = \sum \gamma \times h$

Where:

γ = unit weight of soil

h = height from ground surface

Summation sign denotes the geostatic stress is summed over the individual layers of the soil.

The allowable shear stress is then given by

$\tau = c + \sigma_z k \tan\phi$

Where:

c = cohesion of soil at the location of beam.

ϕ = angle of shearing resistance of soil.

k = coefficient of increase of allowable skin friction due to technology.

The allowable shear force then follows from:

$T_{lim} = OL\tau$

Where:

O = length of perimeter of pile skin.

L = length of pile beam.

3.3.1 Coefficient of Skin Friction

A specific input parameter is the coefficient of skin friction *k* due to applied technology of construction. By default the value of this coefficient is set equal to one. There is no recommendation by standard for its specific value. It has been found from field tests on piles that the value of *k* is usually greater than 1 and may reach the value of 1.5. Theoretically, however, it may attain values even less than 1 (GEO5, User Guide).

3.3.2 Depth of Deformation Zone

The suggested depth of influence is a variable which considerably influences the stiffness of soil below the pile heel. The deeper the influence zone, the smaller the stiffness of subsoil. When the depth of influence zone approaches in the limit zero, the stiffness of subsoil tends to infinity.

The depth of the influence zone depends both on the subsoil parameters and magnitude of the applied surcharge, thus on stress below the pile tip. The GEO5 program for piles assumes that the depth of influence zone is found in the location, where the stress below the tip equals the geostatic stress. Such an idea is illustrated in the following figure:

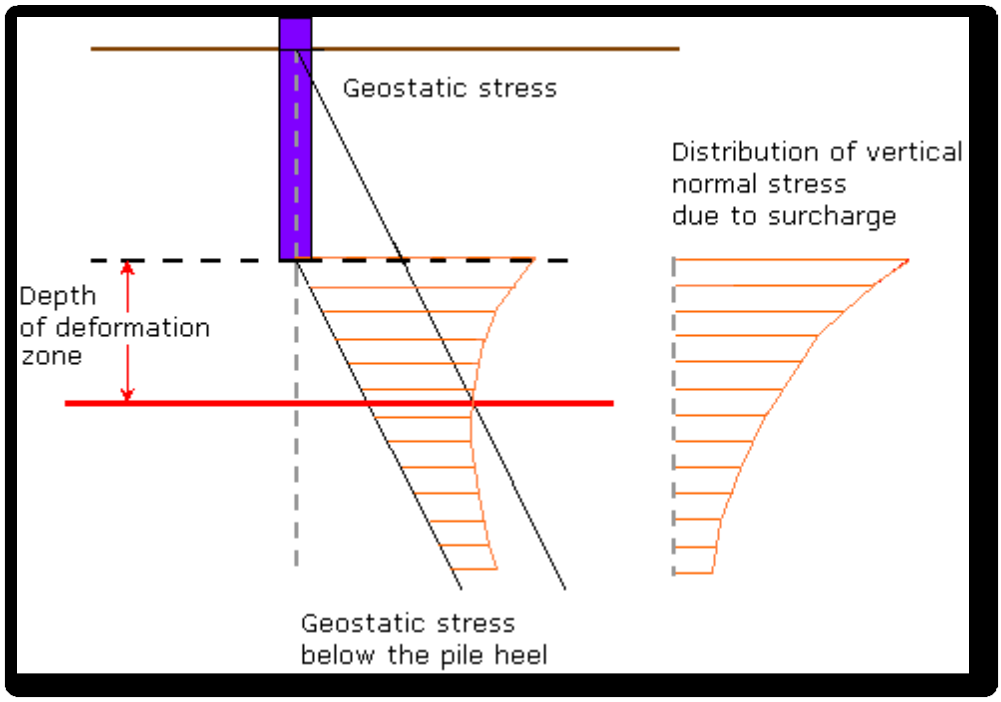

Figure 3.2. Determination of the depth of influence zone below the pile heel (GEO5 User Guide).

3.3.3 Skin Resistance of Pile

The skin resistance of pile is the analysis represented by stiffness of springs supporting individual beams of a pile. This stiffness is associated with material parameters of the Winkler-Pasternak model *C1* and *C2*. The values of *C1* and *C2* are determined from parameter *Edef*, known as the deformation modulus of subsoil. They depend on the depth of influence zone, which varies with the pile deformation (settlement). The variability of influence zone is in the analysis determined such that for zero deformation it receives the value of *1x* the pile diameter and for deformation at the onset of skin failure equals *2,5x* the pile diameter (GEO5, User Guide).

The decisive parameter for the determination of magnitudes of C_1 and C_2 is the deformation Modulus. Caution must be taken when estimating the value of *Edef* from deformational characteristics of soil using standards. In particular, in case of long piles we are essentially dealing with deep seated foundations and the soil at the pile heel will certainly experiences higher stiffness than that proposed by the standard for spread footings. This holds particularly for cohesive soils. The most reliable estimates are of course those obtained directly from experimental measurements.

Formulas given below serve to determine the stiffness of springs representing the shear resistance of pile skin as a function of computed parameters of the elastic subsoil. They depend on the shape of cross-section and for the implemented cross-sections they receive in the form of a circle:

$$k = 2\pi r \sqrt{C_1 \ C_2} \ \frac{K_1(\alpha r)}{K_2(\alpha r)}$$

Where:

r = radius of the pile cross section.

C_1, C_2 = Subsoil Parameters

$K_1(a\ r)$, $K_2(a\ r)$ = Values of the modified Bessel functions.

The parameter α attains the value:

$$\alpha = \sqrt{\frac{C_1}{C_2}}$$

3.3.4 Increments of Vertical Loading

The analyzed pile is loaded gradually in ten increments. The magnitude of load increments in individual steps is determined prior to the actual analysis. In particular, the program searches for such a magnitude of load that causes the pile to exceed the limiting value of settlement specified for the computed limit loading curve (GEO5, User Guide).

3.4 MODEL COMPOSITION

The following criteria were used to create the model:

1) Micropile will be subject to axial compressive loading.
2) Grout will be placed under gravity head only (Type A).
3) Micropile fully bonded along the soil/shaft interface.
4) Micropile will have a uniform cross sectional radius along the interface, yet the dimensions may vary from one test to another.
5) Boundary condition 50 times the pile radius in the lateral direction and 2 times the pile length below tip.
6) Finite Element Method (FEM) will be used to quantify behavior of micropile.
7) Micropile will be tested through three different types of gravelly soils. The geotechnical properties for these soils are indicated in table 3.2 of this present report. The micropile will be embedded either in a single type gravelly soil or through two different types of gravelly soils overlying one another.

8) The unit weight of the grout will be taken at 23kN/m^3 and catalogue standard C 20/25 for concrete will be opted throughout the investigation. For the reinforcement bars, standard catalogue B500 will be used.

Model will be used to study relationships between length (L), diameter (D), slenderness ratio (L/D), and angle of shearing resistance (ϕ) for micropiles embedded in gravelly soils. Present values obtained from the model will then be compared with existing theoretical equations that were discussed in Chapter 2 of this present report.

3.5 NUMERICAL MODEL STEP BY STEP PROCEDURE USING GEO5 FINITE ELEMENT METHOD (FEM)

In order to establish a numerical model capable of generating accurate data, the user in the GEO5 FEM program for piles is ought to fill out a step-by-step procedure that includes several frames, which are the following:

1. **The Project Frame**: This frame serves to input the basic project data and to specify the overall setting of the analysis run. The frame contains an input form to introduce the basic data about the analyzed task: Project general information, the Project description, date and location. The frame also allows the user to choose analysis units from metric to imperial.
2. **The Analysis Method Frame**: This frame provides standards or methods to be used in the analysis of the pile. The user needs to select the type of analysis for the tested pile:

a) Classical theory.

b) Finite Element Method (FEM).

The Finite Element Method (FEM) was chosen throughout this present study.

3. **The Profile Frame**: This frame contains a table with a list of inputted interfaces. The thickness of each individual subsoil layer is indicated in this section. The program allows for raising or lowering the top point of a pile in relevance to the ground level.
4. **The Soils Frame**: This frame contains a table with a list of inserted soils. The table also provides information about currently selected soil displayed in the right part of the frame. The basic soil data needed for the program are the following:

a) Unit weight of soil, γ.

b) Angle of shearing resistance, ϕ.

c) Cohesion, c

d) Void's ratio, v

e) Saturated unit weight, γ_s.

f) Oedometric modulus E_{OD}.

The basic soil data that were inserted for the present load tests are provided in table 3.2 of this current report.

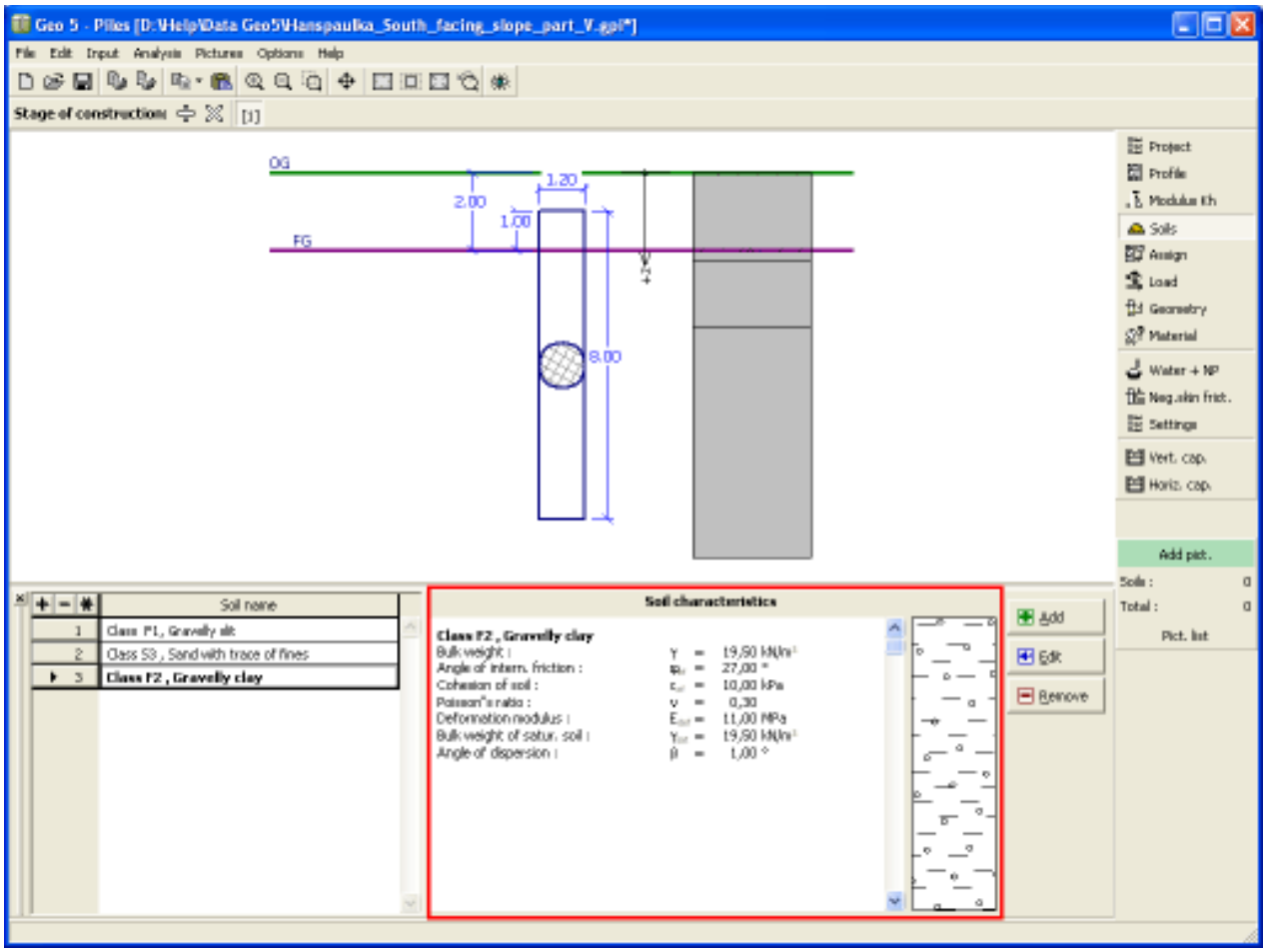

Figure 3.3. Frame (Soils) in GEO5 for piles.

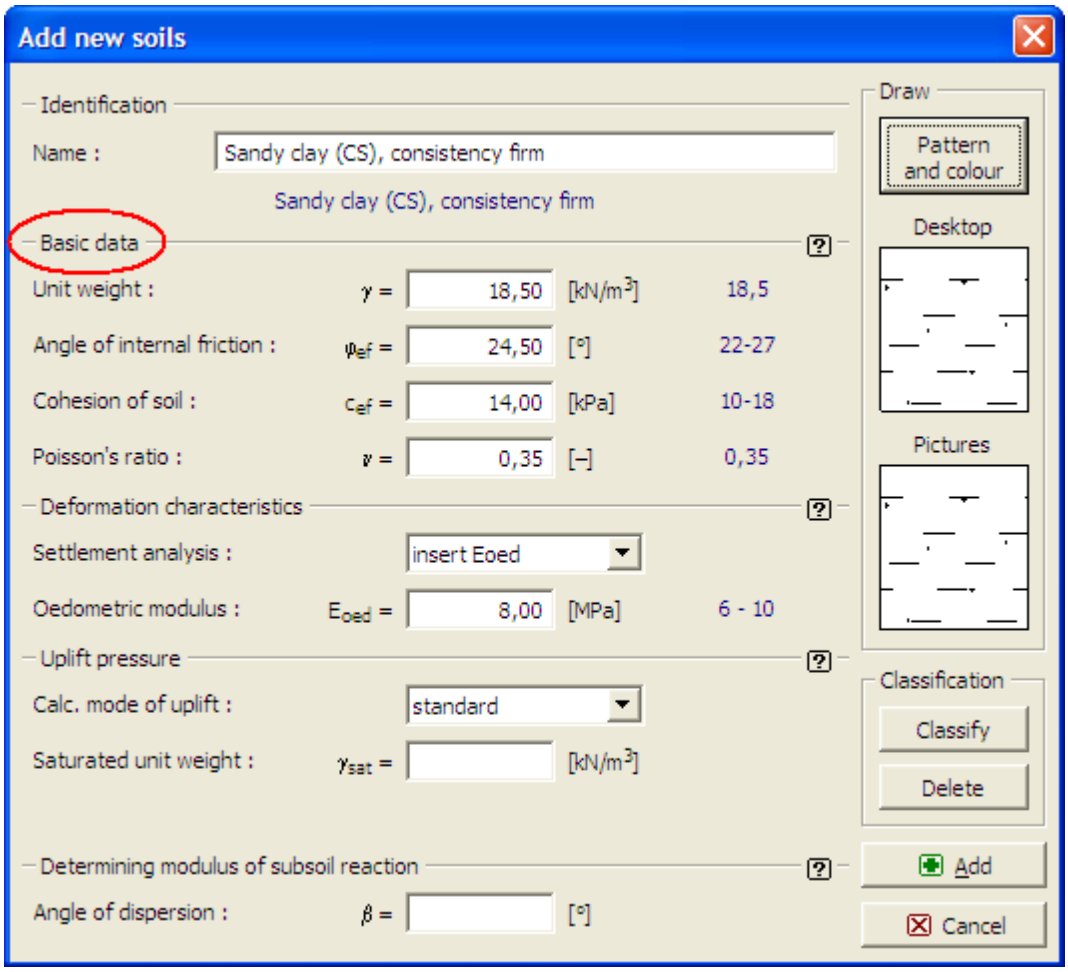

Figure 3.4. Dialogue window for insertion of soil data under the Soils Frame.

5. **The Assign Frame**: The Assign frame contains a list of soil profiles that were constructed in the previous frame. Each profile is graphically represented. The user assigns the soil profile to its respective layer. In this report, the load tests were conducted through three main types of soil profiles:

   a) Silty Gravel (GM).

   b) Gravel with traces of Fines (G-F).

   c) Well Graded Gravel (GW).

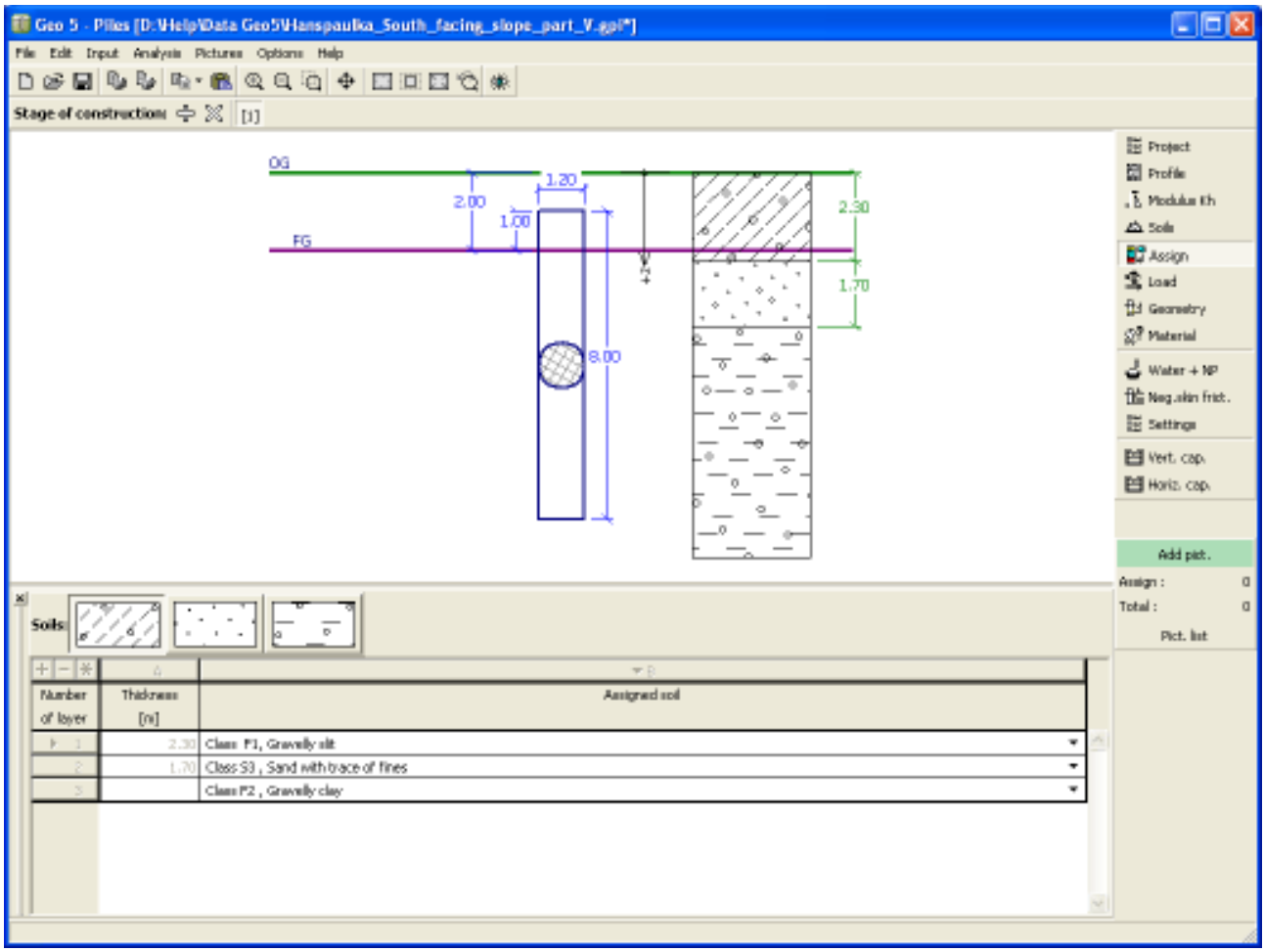

Figure 3.5. Frame “Assign” in GEO5 for piles.

6. **The Load Frame:** This frame contains a table with a list of inputted loads. The user assigns the magnitude and scale of vertical force, the bending moment and the horizontal force. The vertical force was constantly given a magnitude of 500kN for all the load tests that were conducted in this report.

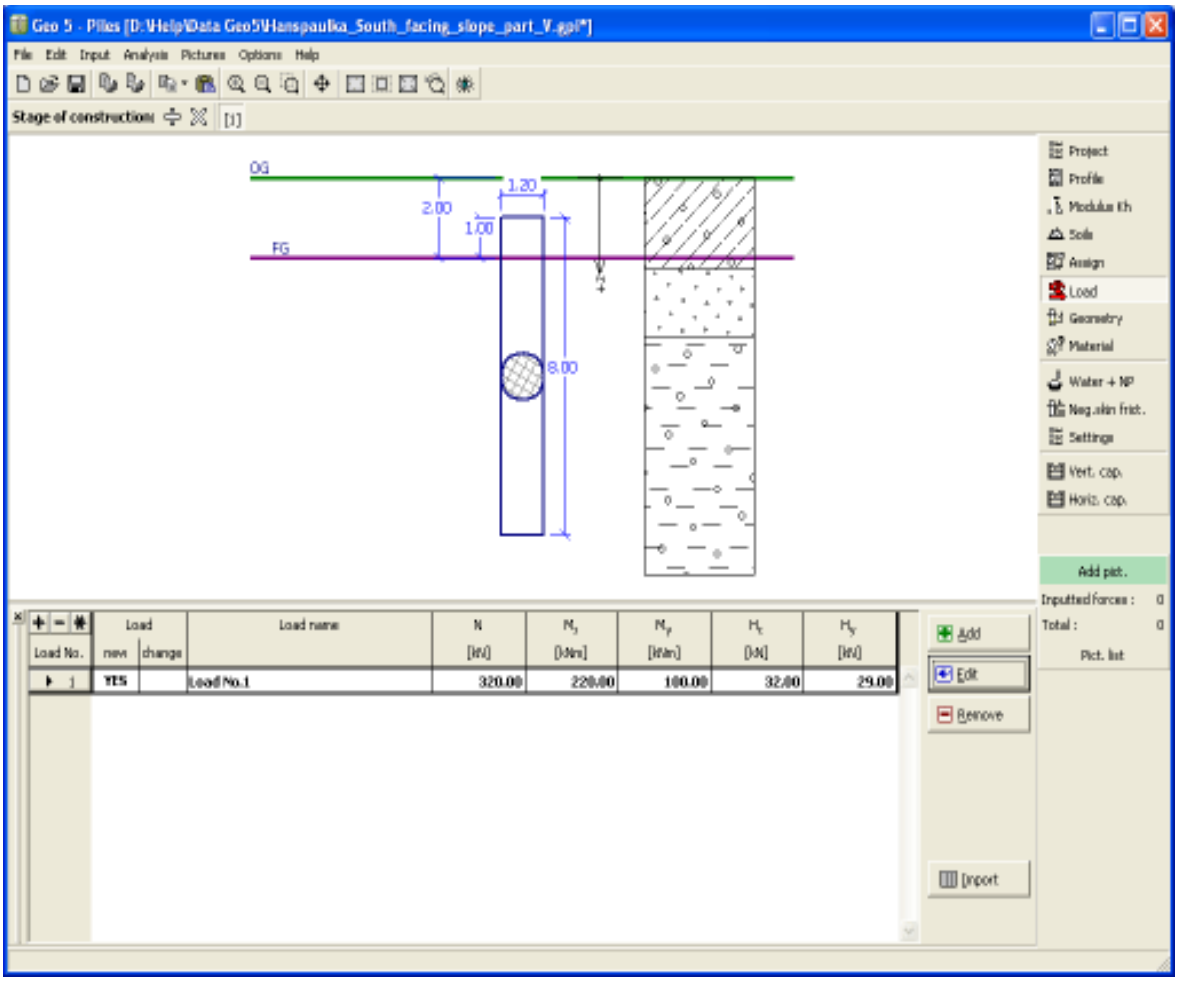

Figure 3.6. The Frame "Load" in GEO5 for piles.

7. **The "Geometry" Frame**: allows for specifying the pile cross-section (circular, variable, rectangle, I-type, cross-section) based on the theory of analysis specified in the Analysis frame. The selected shape with graphic hint is displayed in the central section of the frame. Input fields serve to specify dimensions of the selected cross-section. Cross sectional characteristics are computed by default, but they can also be specified (tubes, hollow cross-sections, steel, I-profiles.

   Given the pile is analyzed using the Finite Element Method, it is possible to account for the influence of pile technology by selecting the specific type of pile or directly by

inputting coefficients. In this study, the cross section of the micropiles testes were circular and the type of pile was chosen to be continuous flight auger Pile

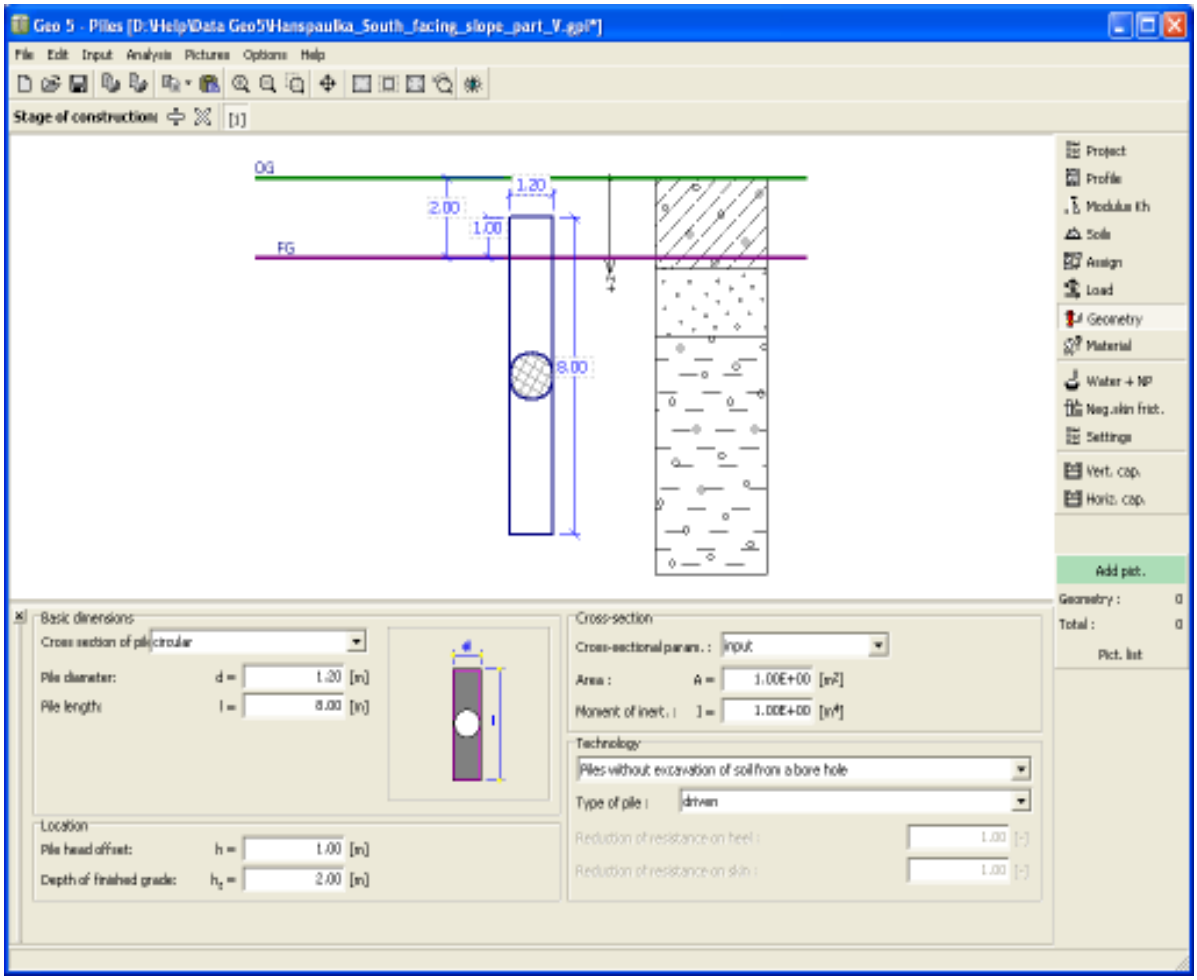

Figure 3.7. The Frame “Geometry” in GEO5 for piles.

8. **The Material Frame**: This frame allows the user to specify the material parameters. The bulk weight of the structure and material of a pile (concrete, timber, steel) are introduced and inputted in this frame.

   The elastic and shear modulus need to be specified when assuming timber or steel piles.

In the case of a concrete pile, the concrete material and the parameters of transverse and longitudinal steel reinforcements are required. The user can either opt to insert the required information manually or choose from the existing catalogue of materials. In this report the unit weight of the grout was taken at 23kN/m^3 and catalogue standard C 20/25 for concrete was taken throughout the investigation. For the reinforcement bars, standard catalogue B500 was taken throughout the report.

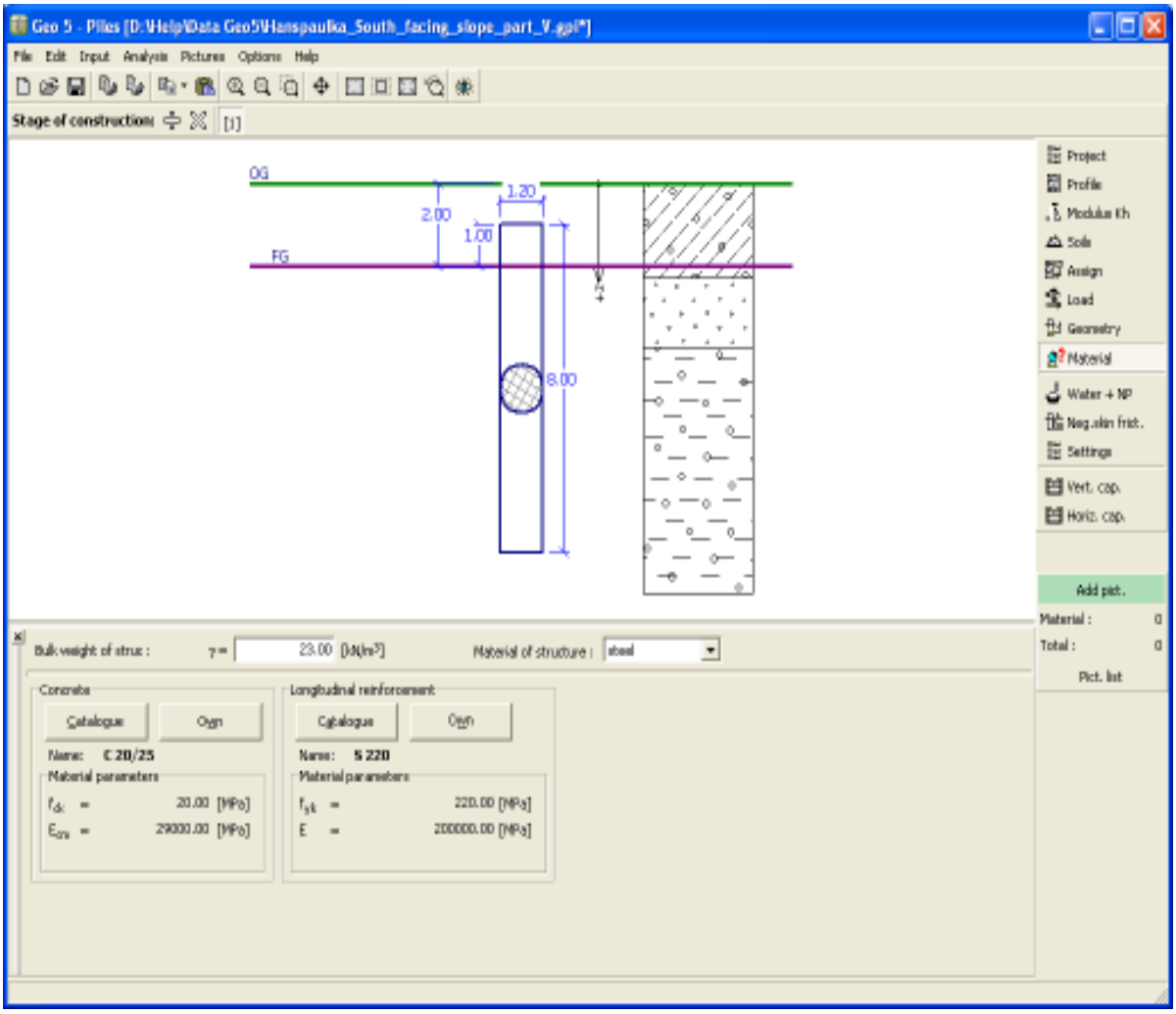

Figure 3.8. The Frame “Meterials” in GEO5 for piles.

9. **The Water Frame**: This frame serves to specify the depth of ground water table. The latter is always in relevance to the ground surface.

10. **The Negative Skin Friction**: This frame serves to specify the settlement of surrounding soil and the depth of influence zone. This frame is only available when the Finite Element Method is selected for analysis. Negative skin friction occurs when the excess pore water pressure held in cohesive soils begins seeping, thus causing the pile to undergo excessive settlements and leading to a downdrag force along the pile's interface. This phenomenon exists in cohesive soils and therefore not covered in this current thesis.

3.6 TYPICAL LOAD DISPLACEMENT RESULTS

The load displacement results describe the variation of vertical carrying capacity load Q as a function of the pile displacement. GEO5 FEM program for piles offers the construction of this curve for the maximal value of settlement equal to 25 mm. This magnitude, however, can be adjusted up to the value of 100 mm before running the calculation. In this report, the load displacement values taken from GEO5 FEM program for piles were plotted in the graph software program DPlot. The graph software program was used to obtain précised load-displacement curves. A typical load-displacement curve for a single micropile embedded in gravelly soil is shown in Figure 3.9.

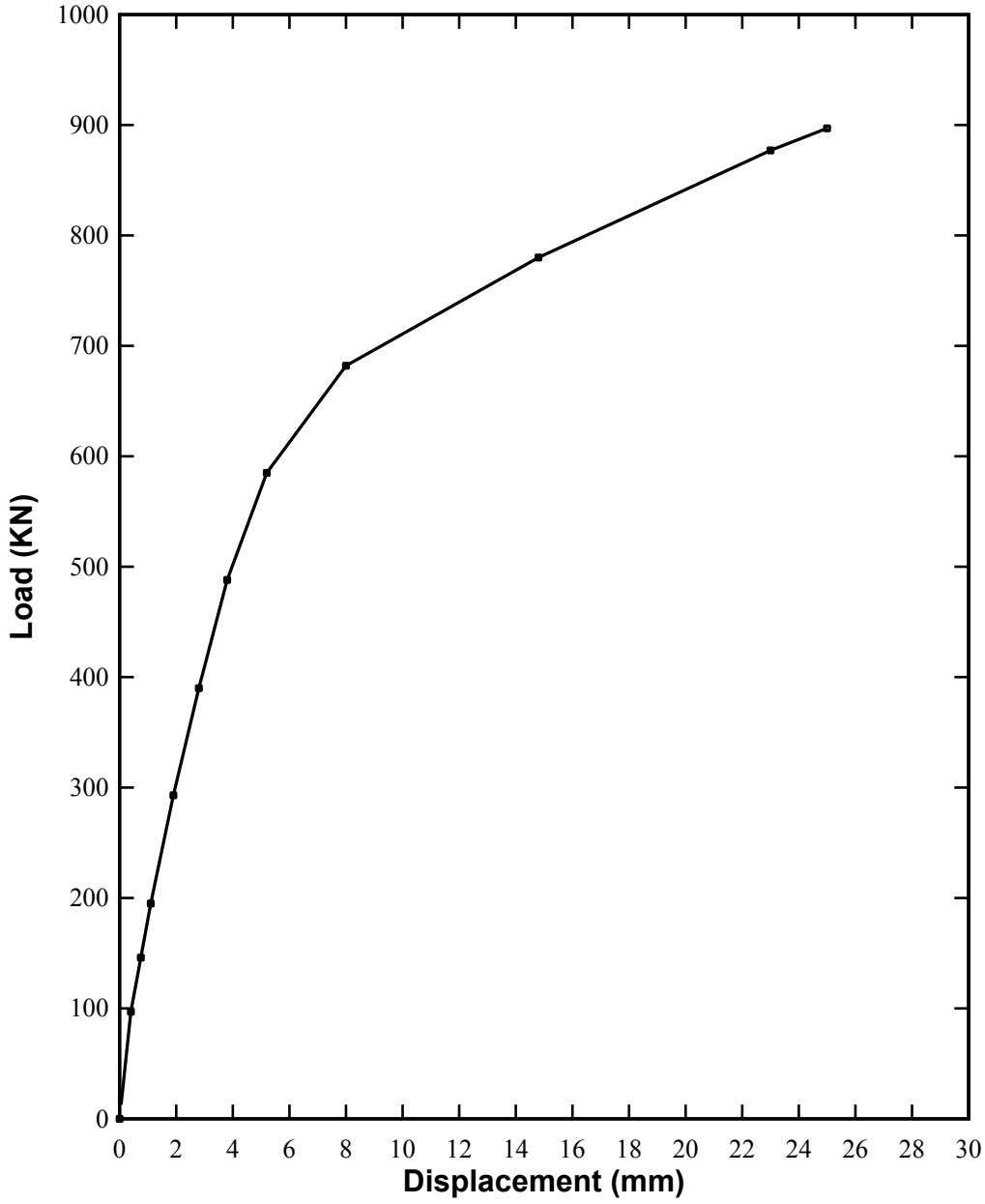

Figure 3.9. Load-Displacement curve for a single micropile embedded in Well Graded Gravel (GW) taken from GEO5 program for piles and plotted through DPLOT.

The load carrying capacity of deep foundations is often assessed through load displacement curves obtained from axial compression and uplift tests. These curves generally exhibit any one of the three shapes show in Figure 3.10 (Hirany and Kulhawy, 1989). Peak A and the asymptote

of B clearly define the ultimate capacity of the foundation in question. However, if the load displacement curve resembles C, the load carrying capacity of the foundation is not clearly defined as the previous two shapes. Load displacement curves for non-displacement foundations (drilled shafts, augercast piles, and micropiles) ideally fall under Curve C (Kulhawy, 2002). The load displacement curves computed for micropiles in GEO5 software perfectly fit criterion C.

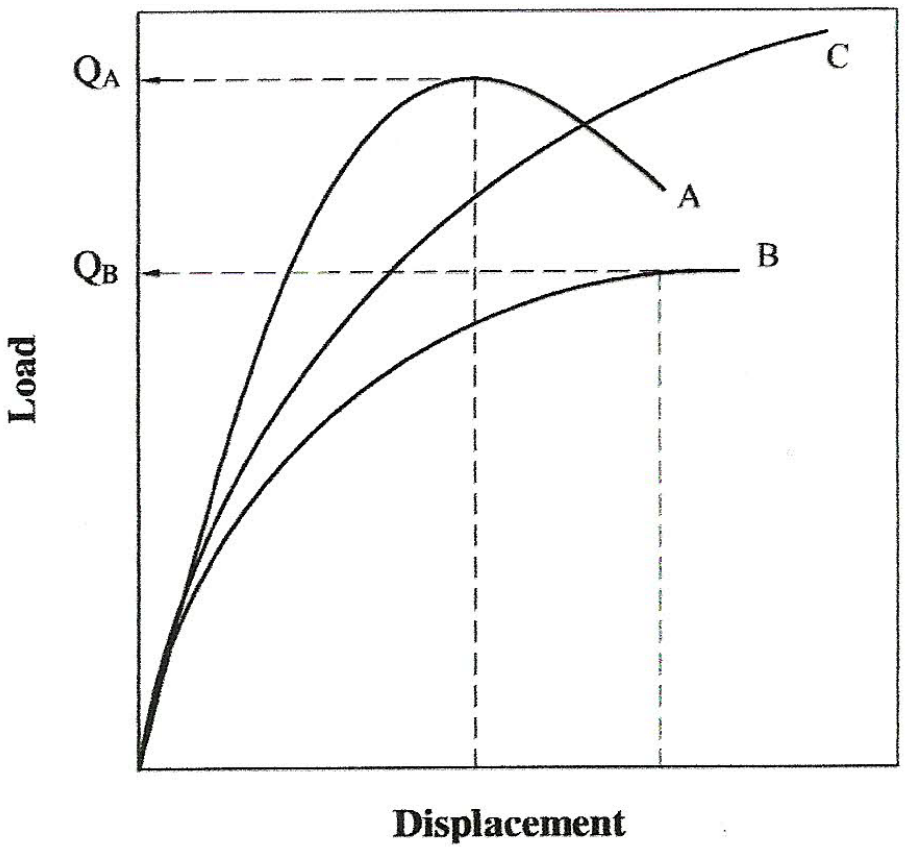

Fig 3.10. Typical load-displacement curves for deep foundations (Kulhawy and Hirany, 2002).

Davisson (1972) proposed a method to define the failure load from the load displacement curve under shape C:

1. Drawn the load-displacement curve.
2. Drawn a tangent line through the initial points of the load-displacement curve.
3. Drawn a line parallel to the tangent line, at an offset equal to 0.15 + D/120 (where D is the pile diameter in inches).
4. The load corresponding to the intersection of the load-displacement curve and this offset is the slop tangent load (L_{st}).

Hirany and Kullhawy (1989, and 2002) suggested that the failure load should be taken at L_2, that is the failure curve threshold that follows when the non-linear load-displacement response occurs. L_{st} and L_2 points are illustrated in Figure 3.11. The L_{st} value falls in the non-linear region, which is considerably very low to regard it as a failure point. Jeon and Kulhawy (2002) conducted several studies on the relationship between L_{st} and L_2 through drilled shafts, augured cast-in-place piles and pressure-injected footings and found that L_2 can be consistently evaluated at 1.18 L_{st}. In this current study, L_2 values will be taken to evaluate the measured capacities.

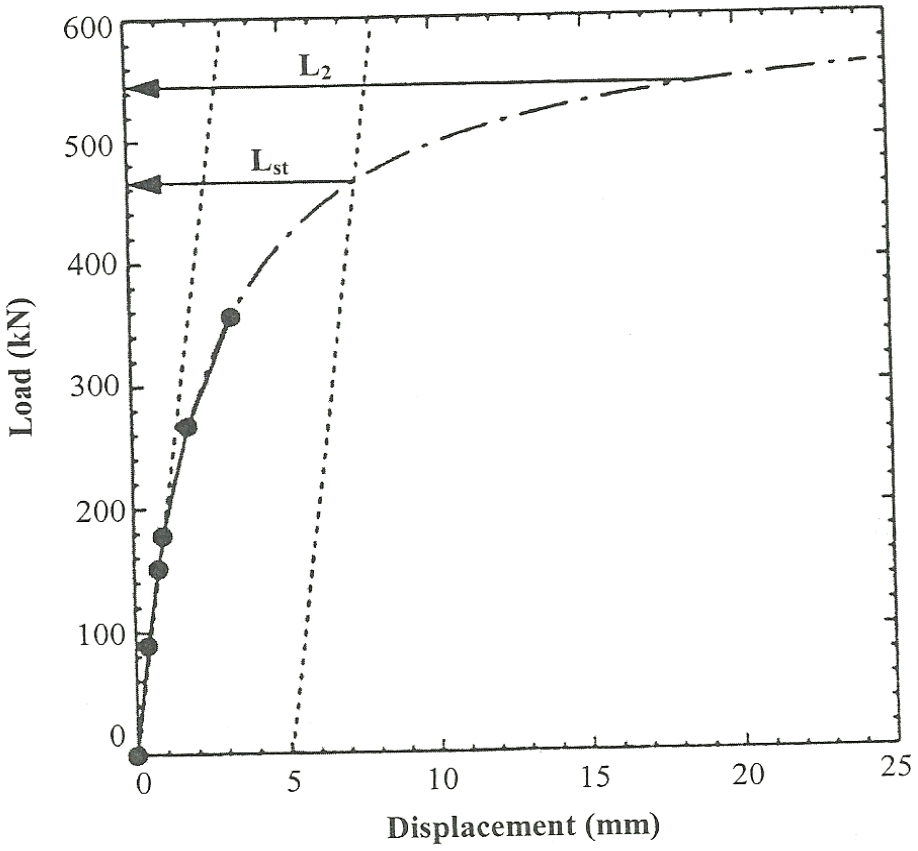

Figure 3.11. Illustration of points L_{ST} and L_2 on a load displacement Curve (Jeon and Kulhaw, 2002).

3.7 MODEL VALIDATION

The numerical model developed in the present study was used to compute the skin friction of micropiles embedded in gravelly soils.

To validate the numerical model, six full-scale field tests taken from three different sites were used for comparison. The site location, micropile type, geotechnical data and failure loads (L_{st}) recorded from the field tests are indicated in table 3.1.

Table 3.1. Comparison of field tests with numerical model obtained from GEO5 FEM program for piles.

1 – Koreck (1978); 2 – Jones and Turner (1980); 3 – (Jeon and Kulhawy, 2002).

Test Site	No.	GWT (m)	Shaft Diameter (m)	Shaft Depth (m)	Load Carrying Length (m)	Pile Type	L_{ST} (kN)	L_{ST} from Model (kN)	Error %
Germany[1]	1	3.9	0.18	8	8	D	578	509	12
Germany	2	3.9	0.18	10	10	D	476	581	-22
Germany	3	4.7	0.15	16	5	D	979	860	12
Westbourne, UK[2]	4	-	0.15	9	9	D	329	312	5
Coney Island, NY[3]	5	1.2	0.17	10.7	3	B	347	295	15
Coney Island, NY	6	1.2	0.19	13.7	6.1	B	472	443	6

The soil parameters taken from the field tests (unit weight of soil (γ), the angle of shearing resistance of soil (ϕ), cohesion (c), coefficient of lateral Erath Pressure at rest (K_0), void's ratio (v), the saturated unit weight (γ_s) and the groundwater depth) were executed in the numerical model and the results were used for validation. The slope tangent values (L_{st}) for the numerical model were obtained from the load-displacement curves using Jeon and Kulhawy's method (2002). Failure loads (L_{st}) values obtained from the Numerical Model are included in table 3.1.

The results revealed in Table 3.1 show reasonable agreements between the field tests and the Numerical Model results. In test 4, a marginal error of 22% could be due from the overvalued soil parameters assumed in some cases by the authors (Jeon and Kulhawy, 2002).

3.8 MODEL TEST RESULTS

The Numerical Model obtained from the program GEO5 Finite Element Method for piles was successfully validated. The model was then used to generate data for a broad range of parameters. The micropiles were embedded in three different types of gravelly soils: Silty Gravel (GM), Gravel with traces of Fines (G-F) and Well Graded Gravel (GW). The first nine tests were conducted in single layered gravelly soils, while the twenty-one others were conducted in multi-layered gravelly soils. The length, diameter and slenderness ratio (L/D) were modified on several occasions to examine the dimensional effects. In total, 30 load test data were carefully examined. The soil layers applied in the tests, including the geotechnical properties and the load test results are provided in table 3.2 and 3.3, respectively. For analysis purposes, the soil layers were divided into three main categories: Well Graded Gravel (GW), Gravel with traces of Fines (G-F) and Silty Gravel (GM) based on the Unit Soil Classification System.

Table 3.2.Geotechnical properties of tested soils.

Soil Properties							
Soil Characteristics	**(γ) kN/m^3**	**(ϕ) (^{o})**	**c (kPa)**	**ν**	**E (Mpa)**	**(γ_s) kN/m^3**	**Gravel %**
Well Graded Gravel (GW)	21	40	0	0.2	450	22	60-75%
Gravel with traces of Fines (G-F)	19	35	0	0.2	120	20.	55-60
Silty Gravel (GM)	19	3	0	0.3	95	20.5	40-45

Table 3.3. Load test data generated from GEO5 FEM for piles.

									Present		Backcalculated
Test	Type(s)	Thickness of layer(s)		Pile (L)	Pile (D)	Slenderness Ratio	Applied Load	Parametric Area	Failure Load L_{st}	Failure Load L_2	Skin Friction (f_s)
No.	of Soil(s)	H1 (m)	H2 (m)	(m)	(m)	(L/D)	(kN)	(m^2)	(kN)	(kN)	(kPa)
1	(GW)	10.00	-	10.00	0.20	50.00	500.00	6.28	678	800	**127**
2	(GW)	14.00	-	14.00	0.20	70.00	500.00	8.80	1200	1416	**161**
3	(GW)	16.00	-	16.00	0.20	80.00	500.00	10.05	1390	1640	**164**
4	(G-F)	10.00	-	10.00	0.20	50.00	500.00	6.28	490	578	**92**
5	(G-F)	14.00	-	14.00	0.20	70.00	500.00	8.80	845	996	**113**
6	(G-F)	16.00	-	16.00	0.20	80.00	500.00	10.05	1126	1329	**132**
7	(GM)	10.00	-	10.00	0.20	50.00	500.00	6.28	404	476	**76**
8	(GM)	14.00	-	14.00	0.20	70.00	500.00	8.80	743	877	**100**
9	(GM)	16.00	-	16.00	0.20	80.00	500.00	10.05	854	1108	**111**
10	(GM) / (GW)	5.00	5.00	10.00	0.20	50.00	500.00	6.28	623	735	**117**
11	(GM) / (GW)	7.00	7.00	14.00	0.20	70.00	500.00	8.80	1140	1345	**153**
12	(GM) / (GW)	8.00	8.00	16.00	0.20	80.00	500.00	10.00	1330	1570	**157**
13	(GM) / (G-F)	5.00	5.00	10.00	0.20	50.00	500.00	6.28	475	560	**89**
14	(GM) / (G-F)	7.00	7.00	14.00	0.20	70.00	500.00	8.80	801	946	**108**
15	(GM) / (G-F)	8.00	8.00	16.00	0.20	80.00	500.00	10.00	1085	1286	**129**

									Present		Backcalculated
Test	Type(s)	Thickness of layer(s)		Pile (L)	Pile (D)	Slenderness Ratio	Applied Load	Parametric Area	Failure Load L_{st}	Failure Load L_2	Skin Friction (f_s)
No.	of Soil(s)	H1 (m)	H2 (m)	(m)	(m)	(L/D)	(kN)	(m^2)	(kN)	(kN)	(kPa)
16	(G-F) / (GW)	5.00	5.00	10.00	0.20	50.00	500.00	6.28	638	753	**120**
17	(G-F) /	7.00	7.00	14.00	0.20	70.00	500.00	8.80	1156	1364	**155**
18	(G-F) / (GW)	8.00	8.00	16.00	0.20	80.00	500.00	10.00	1378	1580	**158**
19	(GW)	14.00	-	14.00	0.16	87.50	500.00	7.04	930	1098	**156**
20	(GW)	14.00	-	14.00	0.24	58.33	500.00	10.56	1480	1746	**165**
21	(G-F)	14.00	-	14.00	0.16	87.50	500.00	7.04	660	779	**111**
22	(G-F)	14.00	-	14.00	0.24	58.33	500.00	10.56	1102	1300	**123**
23	(GM)	14.00	-	14.00	0.16	87.50	500.00	7.04	551	650	**92**
24	(GM)	14.00	-	14.00	0.24	58.33	500.00	10.56	913	1077	**102**
25	(GM) / (GW)	7.00	7.00	14.00	0.16	87.50	500.00	7.04	673	794	**113**
26	(GM) / (GW)	7.00	7.00	14.00	0.24	58.33	500.00	10.56	1387	1637	**155**
27	(GM) / (G-F)	7.00	7.00	14.00	0.16	87.50	500.00	7.04	608	717	**102**
28	(GM) / (G-F)	7.00	7.00	14.00	0.24	58.33	500.00	10.56	1032	1218	**115**
29	(G-F) / (GW)	7.00	7.00	14.00	0.16	87.50	500.00	7.04	772	911	**129**
30	(G-F) / (GW)	7.00	7.00	14.00	0.24	58.33	500.00	10.56	1405	1658	**157**

3.9 PARAMETRIC STUDY

As mentioned earlier, the ratio of circumference to the cross sectional area in micropiles is very high, hence their capacities rely fundamentally on the parametric area. The end bearing capacity is negligible.

The Length (L), the Diameter (D) and the slenderness ratio (L/D) are expected to have a direct impact on the capacity of the micropile. A direct increase in the Length (L) should anticipate a direct increase in the capacity of the micropile. The latter is primarily due to an increased load carrying length which thus results in an increased effective stress. Increasing the Diameter (D) of the micropile should have a similar outcome.

3.9.1 Effect of Length (L)

In micropiles embedded in well graded Gravel ($\phi = 40^0$), an increase in the length (L) and slenderness ratio (L/D) resulted in a noticeable increase in the ultimate unit skin friction, as revealed in figure 3.12. For a 60% length increase of L=10m to L=16m with a constant diameter, the ultimate unit skin friction (f_s) increased from 127kPa to 164kPa, thus an elevation of 30%.

For micropiles embedded in Gravel with traces of Fines (G-F), the results reveal an increase of 44% in ultimate unit skin friction (f_s) following a 60% increase in length with constant diameter. As for Silty Gravel, the same increase in length resulted in a 46% increase in the ultimate unit skin friction (f_s).

Overall, the results reveal that an increase in length (L), which accompanies an increase in slenderness ratio (L/D) results in a significant increase of the ultimate unit skin friction (f_s). The

latter revealed a lower impact with an increasing Gravel content. This could be explained from the dilatant behavior of gravelly soils, which tends to rise with an increase in the gravel content.

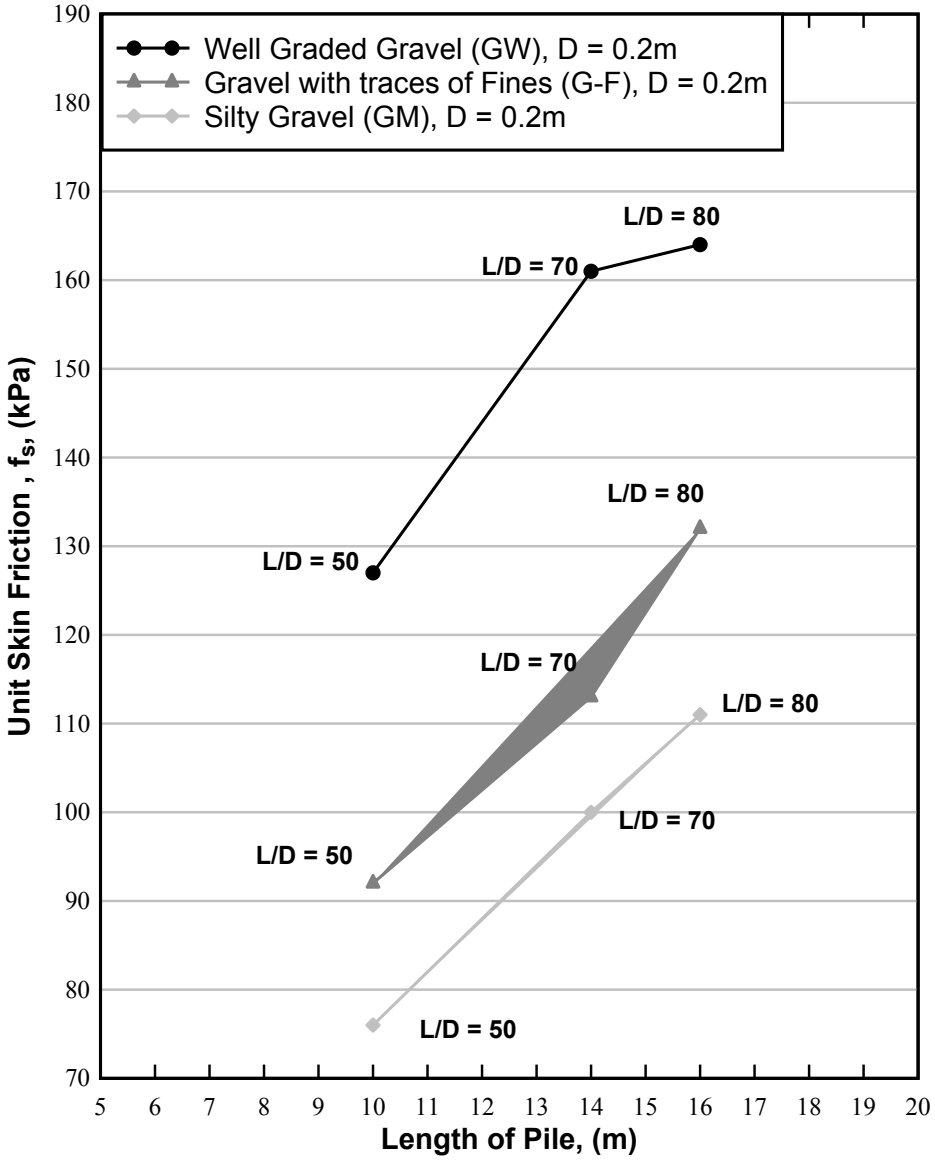

Figure 3.12. Length of Micropile vs. Unit Skin Friction in uniform gravelly soils.

For micropiles embedded in multi-layered gravelly soils, similar trends were noticed. With a 60% increase in the length and given a constant pile diameter of 0.2m, micropiles embedded in Silty Gravel (GW) overlying Gravel with traces of Fines (G-F) recorded the highest increase in

ultimate unit skin friction with 45%. Compared to 34% increase for Silty Gravel (GM) overlying Well graded Gravel (GW) and 32% for Gravel with traces of Fines (G-F) overlying Well graded Gravel (GW).

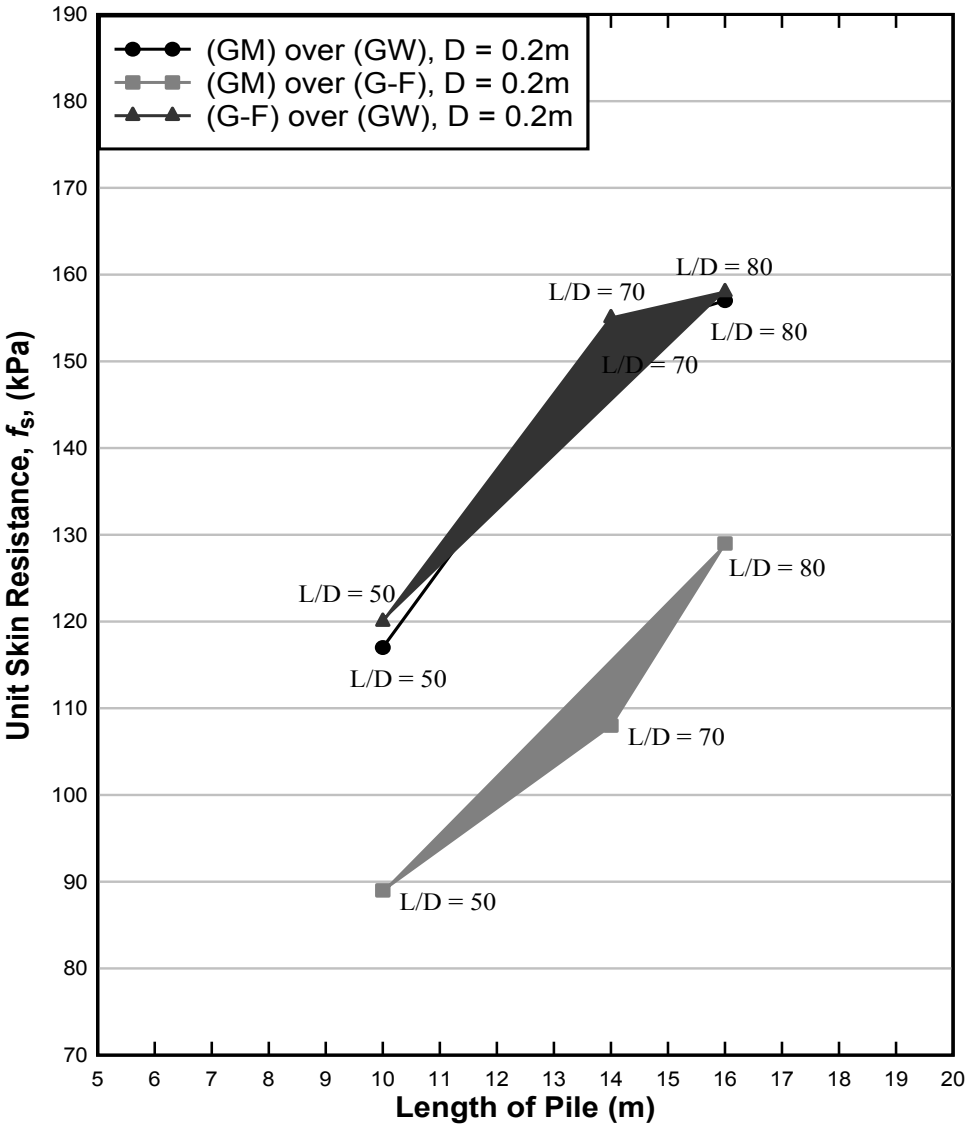

Figure 3.13. Length of Micropile vs. Unit Skin Friction in multi layered gravelly soils.

3.9.2 Effect of Diameter (D)

Figure 3.14 and 3.15 reveal the effect of diameter (D) on the ultimate unit skin friction f_s for micropiles embedded in uniform and multi-layered gravelly soils, respectively. The results illustrate modest effects when compared to the influence of length (L). Given a constant length, increasing the diameter of the micropile which automatically reduces the slenderness ration (L/D) results in a moderate increase of the ultimate unit skin friction f_s for gravelly soils.

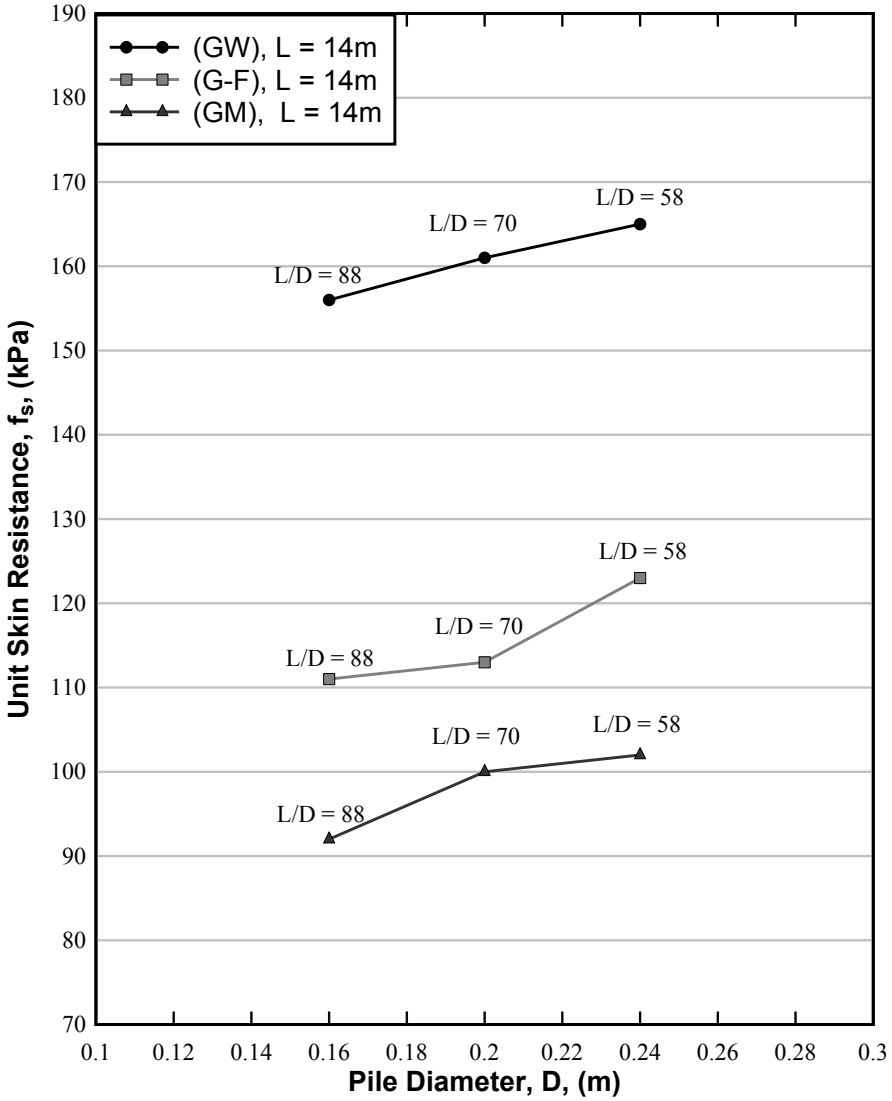

Figure 3.14. Diameter of Micropile vs. Unit Skin Friction in uniform gravelly soils.

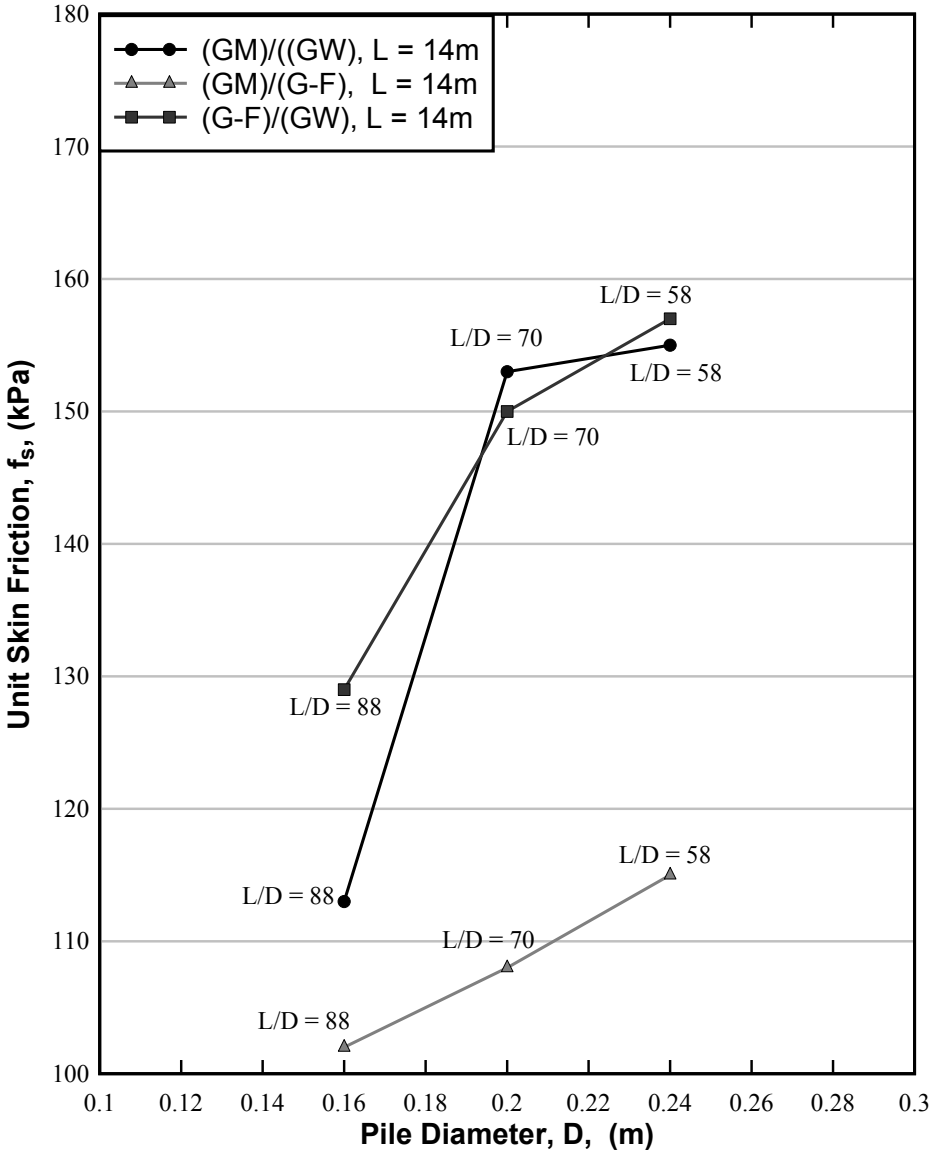

Figure 3.15. Diameter of Micropile vs. Unit Skin Friction in multi-layered gravelly soils.

The rise of the ultimate unit skin friction f_s depends on the parameters L and D. With a constant D, increasing L of which directly increases the slenderness ratio (L/D) results in higher f_s values. With a constant L, increasing D of which directly decreases the slenderness ratio (L/D) results in high f_s values as well.

3.10 ANGLE OF SHEARING RESISTANCE OF SOIL ϕ

The angle of shearing resistance of soil (ϕ) is expected to contribute heavily on the skin friction. The embedded soil is cohesionless and therefore its resistance relies, according to Mohr-Coulomb, on vertical effective stress σ' and the tangent of the angle of shearing resistance of soil tan ϕ.

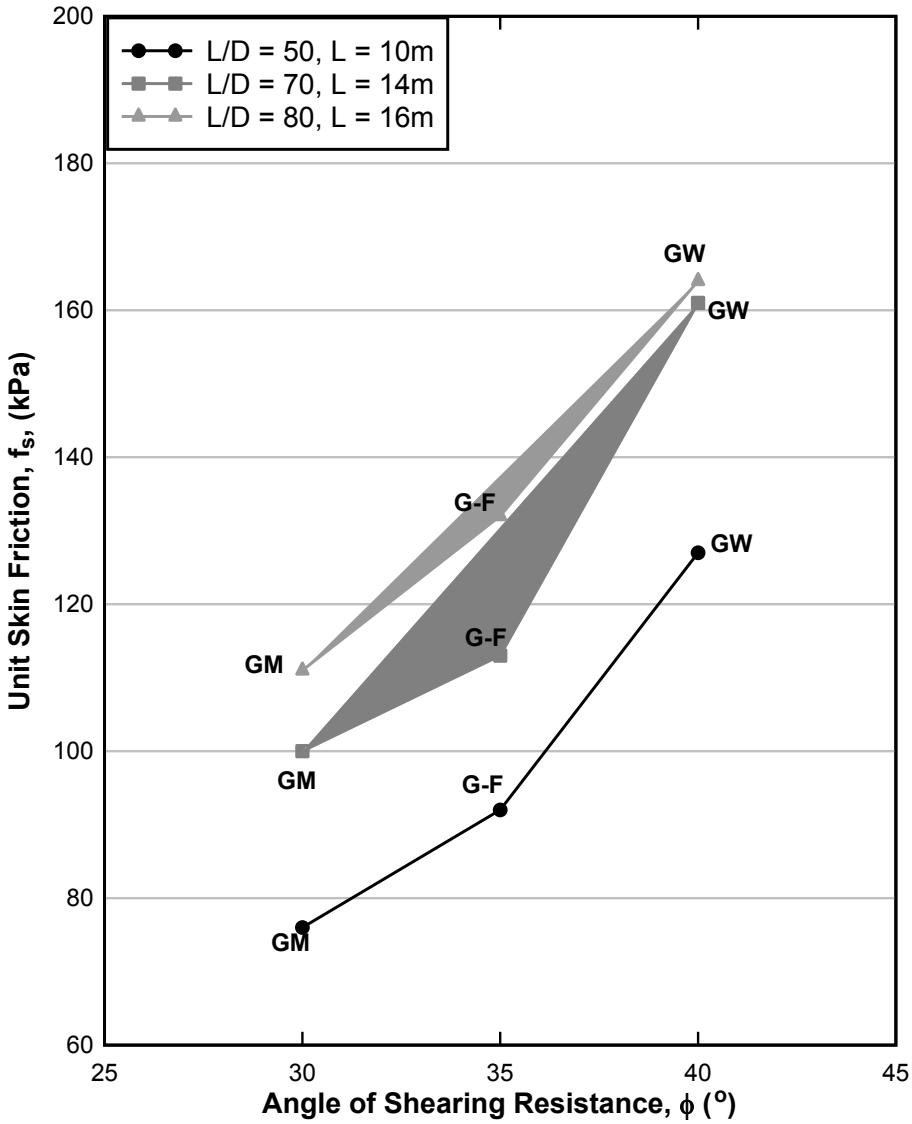

Figure 3.16. Angle of shearing resistance vs. Unit Skin Friction for uniform gravelly soils.

Figure 3.16 and 3.17 reveal the impact of the angle of shearing resistance of soil on the ultimate unit skin friction f_s. For a slenderness ratio (L/D) of 50, an increase of 21% in the ultimate unit skin friction f_s was noticed from $\phi = 30^0$ to $\phi = 35^0$, while a significant increase of 67% was recorded from $\phi = 30^0$ to $\phi = 40^0$. For slenderness ratio (L/D) of 70, an increase of 13% was recorded between $\phi = 30^0$ and $\phi = 35^0$ and 61% between $\phi = 30^0$ and $\phi = 40^0$. For slenderness ratio (L/D) of 80, the ultimate skin friction f_s recorded an increase of 19% between $\phi = 30^0$ and $\phi = 35^0$ and 48% between $\phi = 30^0$ and $\phi = 40^0$. It is safe to state that an increase in the angle of shearing resistance of soil for micropiles embedded in gravelly soils would result in an increase in the ultimate unit skin friction f_s and ultimate skin friction capacity Q_s. With higher slenderness ratio (L/D), the increase in ultimate unit skin friction f_s was less apparent.

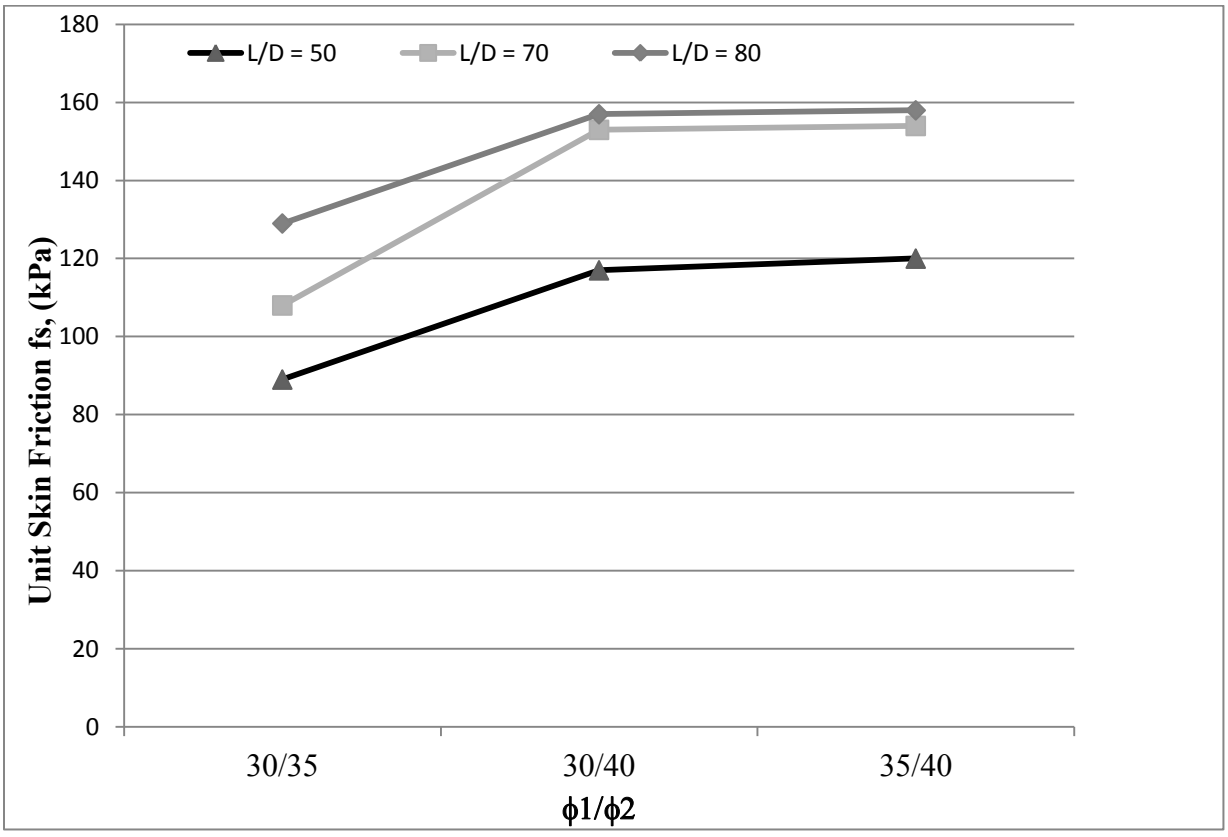

Figure 3.17. Angle of shearing resistance vs. Unit Skin Friction for multi layered gravelly soils.

3.11 THEORY

According to Bruce and Juran (1997b), the load carrying capacity Q is given by

$$Q = Q_s + Q_p \qquad (1)$$

Where

Q_s = Ultimate skin friction capacity.

Q_p = End bearing capacity.

As explained earlier, the ratio of circumference to the cross sectional area in micropiles is very high, hence End Bearing capacity becomes negligible and the load carrying capacity equation becomes

$$Q = Q_s \qquad (2)$$

Several authors evaluated ultimate skin friction capacity of drilled shafts through design equations. According to Meyerhof (1976), Reese and O'Neill (1988), Kulhawy (1991) and Hassan and O'Neill (1994), the ultimate skin friction capacity Q_s is given by the following equation

$$Q_s = f_s \times A_s \qquad (3)$$

Where:

f_s = ultimate unit skin friction of soil.

A_s= surface area of shaft producing skin friction.

Reese and O'Neill (1988) provided an empirical method based on a set of 41 drilled shaft loads. The ultimate unit skin friction in sand is given by

$f_s = \beta\sigma'_z \leq 200$ kPa limit (5)

Where:

σ'_z = vertical effective stress in soil at depth z.

β = proportionality coefficient that depends on various factors, including construction techniques, soil characteristics, and particularly the initial state of stress characterized by the ambient coefficient of earth pressure at rest, K_o. Reese and O'Neill (1988) recommended coefficient to be

$\beta = 1.5 - 0.245\, z^{0.5}$, (6)

With limits of $1.2 \geq \beta \geq 0.25$, where z = depth below ground surface (m).

O'Neill and Hassan (1994) suggested an empirical relationship between β values and the SPT blow count N. The β in sand is hence provided by the following equation

For $N \geq 15$ $\beta_{nominal} = 1.5 - 0.42\,[z\,(m)]^{0.34}$, $1.2. \geq \beta \geq 0.25$ (7)

For $N < 15$ $\beta = \beta_{nominal}\, N/15$

Kulhawy (1991) provided a method based on soil properties. The ultimate unit skin friction is hence given by the following equation:

$f_s = \sigma'_z K \tan\delta$ (8)

Where:

K = coefficient of lateral earth pressure.

δ = effective stress angle of friction for the soil-shaft interface.

Kulhawy (1991) suggested that δ can be expressed as a fraction of the angle of shearing resistance of soil ϕ. With good slurry conditions and sound construction methods, a rough skin develops along soil/pile interface, and hence δ/ϕ would be equal to 1.0. Poor slurry conditions could make the ratio 0.8 or lower. In this thesis, the ratio is assumed to be 1.0.

The coefficient of lateral earth pressure K is a function of the original in situ horizontal stress coefficient K_0. As indicated in chapter 3, Mayne and Kulhawy (1982) provided a relationship to determine K_0 based on the angle of shearing resistance of soil ϕ and the overconsolidation ratio (OCR) using the following equation

$$K_0 = (1 - \sin\phi)\, OCR^{\sin\phi}$$

Table 3.4. Typical values for angle of shearing resistance of soil and Overconsolidation Ratio (Jeon and Kulhawy, 2002).

Soil Type	**ϕ (deg)**	**OCR**
Loose Sand	28-32	1-3
Medium Dense Sand	32-38	3-10
Dense Sand, Gravel	38-45	10-20

The lateral earth pressure K were computed as suggested by Rollins et al. (2005), by the equation

$$K = 4.62\ e^{(-0.137z)} \qquad (9)$$

Where

z = depth below ground surface.

The lateral earth pressure K was modified to accommodate for drilled shafts embedded in gravelly soils. The lateral earth pressure K values for Kulhawy's method will be taken from equation (9) of this present report.

The above noted theories will be examined and compared with the present capacities from the numerical model.

3.12 COMPARISON OF PRESENT AND COMPUTED CAPACITIES

Existing theories for drilled shafts in cohesionless soils were compared with the present capacities from the load-displacement curves obtained through the numerical model. Ultimate unit capacity Q_{L1} was measured from the Davisson method (1972) and was multiplied by a factor 1.8 to give Q_{L2}. Q_{L2} loads were chosen for the Present values. Figure 3.18 shows a typical load displacement curve taken from test no.1 of this current study.

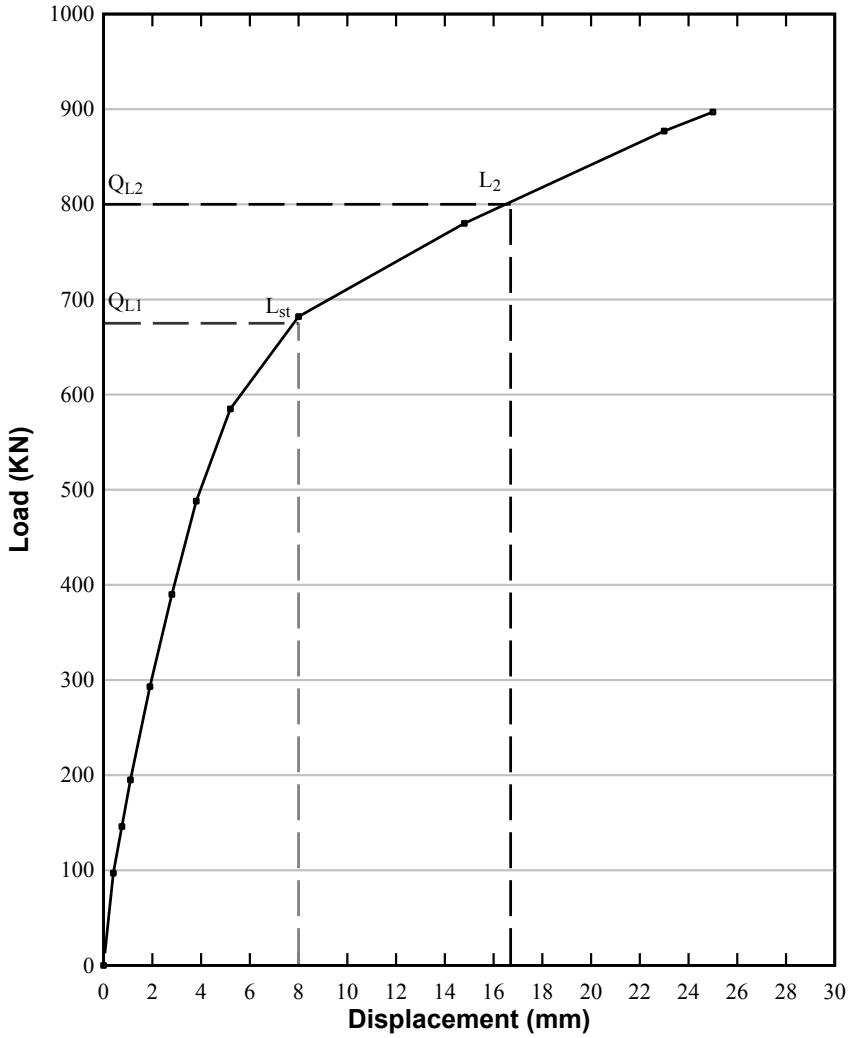

Figure 3.18. Load-Displacement curve for Test no.1.

					Present Calculations			Computed Calculations		
Test No.	Type(s) of soils	Pile (L) (m)	Pile (D) (m)	Slenderness Ratio (L/D)	Failure Load L_{st} (kN)	Failure Load L_2 (kN)	(f_s) from Q_{L2} (kPa)	Reese and O'Neill (1988) (kPa)	Hassan and O'Neill (1994) (kPa)	Rollins et al. (2005) (kPa)
1	(GW)	10.00	0.20	50.00	678.00	800.00	127.00	152.00	122.00	207.00
2	(GW)	14.00	0.20	70.00	1200.00	1416.00	161.00	172.00	138.00	166.00
3	(GW)	16.00	0.20	80.00	1390.00	1640.00	164.00	175.00	141.00	145.00
4	(G-F)	10.00	0.20	50.00	490.00	578.00	92.00	138.00	110.00	155.00
5	(G-F)	14.00	0.20	70.00	845.00	996.00	113.00	155.00	125.00	126.00
6	(G-F)	16.00	0.20	80.00	1126.00	1329.00	132.00	158.00	128.00	106.00
7	(GM)	10.00	0.20	50.00	404.00	476.00	76.00	138.00	110.00	129.00
8	(GM)	14.00	0.20	70.00	743.00	877.00	100.00	155.00	125.00	103.00
9	(GM)	16.00	0.20	80.00	854.00	1108.00	111.00	158.00	128.00	88.00
10	(GM) / (GW)	10.00	0.20	50.00	623.00	735.00	117.00	145.00	116.00	167.00
11	(GM) / (GW)	14.00	0.20	70.00	1140.00	1345.00	153.00	162.00	132.00	134.00
12	(GM) / (GW)	16.00	0.20	80.00	1330.00	1570.00	157.00	166.00	134.00	117.00
13	(GM) / (G-F)	10.00	0.20	50.00	475.00	560.00	89.00	138.00	110.00	142.00
14	(GM) / (G-F)	14.00	0.20	70.00	801.00	946.00	108.00	155.00	125.00	115.00
15	(GM) / (G-F)	16.00	0.20	80.00	1085.00	1286.00	129.00	158.00	128.00	97.00
16	(G-F) / (GW)	10.00	0.20	50.00	638.00	753.00	120.00	145.00	116.00	181.00

					Present Calculations			Computed Calculations		
Test No.	Type(s) of Soil(s)	Pile (L)	Pile (D)	Slenderness Ratio	Failure Load Q_{L1}	Failure Load Q_{L2}	(f_s) from Q_{L2}	Reese and O'Neill (1988)	Hassan and O'Neill (1994)	Rollins et al. (2005)
		(m)	(m)	(L/D)	(kN)	(kN)	(kPa)	(kPa)	(kPa)	(kPa)
17	(G-F) / (GW)	14.00	0.20	70.00	1155.00	1364.00	155.00	163.00	132.00	146.00
18	(G-F) / (GW)	16.00	0.20	80.00	1378.00	1580.00	158.00	166.00	134.00	126.00
19	(GW)	14.00	0.16	87.50	930	1098	156	172.00	138.00	166.00
20	(GW)	14.00	0.24	58.33	1480	1746	165	172.00	138.00	166.00
21	(G-F)	14.00	0.16	87.50	660	779	111	155.00	125.00	126.00
22	(G-F)	14.00	0.24	58.33	1102	1300	123	155.00	125.00	126.00
23	(GM)	14.00	0.16	87.50	551	650	92	155.00	125.00	103.00
24	(GM)	14.00	0.24	58.33	913	1077	102	155.00	125.00	103.00
25	(GM)/ (GW)	14.00	0.16	87.50	673	794	113	162.00	132.00	134.00
26	(GM)/ (GW)	14.00	0.24	58.33	1387	1637	155	162.00	132.00	134.00
27	(GM) / (G-F)	14.00	0.16	87.50	608	717	102	155.00	125.00	115.00
28	(GM) / (G-F)	14.00	0.24	58.33	1032	1218	115	155.00	125.00	115.00
29	(G-F) / (GW)	14.00	0.16	87.50	772	911	129	163.00	132.00	181.00
30	(G-F) / (GW)	14.00	0.24	58.33	1405	1658	157	163.00	132.00	181.00

Table 3.5.Test Results for Present and Computed Capacities.

Test	Type(s)	Failure Load L_{st}	Failure Load L_2	Reese and O'Neill (1988)	Hassan and O'Neill (1994)	Rollins et al. (2005)
No.	of Soil(s)	(kN)	(kN)	(kN)	(kN)	(kN)
1	(GW)	678	800	955	766	1300
2	(GW)	1200	1416	1513	1214	1460
3	(GW)	1390	1640	1750	1410	1450
4	(G-F)	490	578	867	691	973
5	(G-F)	845	996	1364	1100	1109
6	(G-F)	1126	1329	1580	1280	1060
7	(GM)	404	476	867	691	810
8	(GM)	743	877	1364	1100	906
9	(GM)	854	1108	1580	1280	880
10	(GM) / (GW)	623	735	911	729	1049
11	(GM) / (GW)	1140	1345	1426	1162	1179
12	(GM) / (GW)	1330	1570	1660	1340	1170
13	(GM) / (G-F)	475	560	867	691	892
14	(GM) / (G-F)	801	946	1364	1100	1012
15	(GM) / (G-F)	1085	1286	1580	1280	970
16	(G-F) / (GW)	638	753	911	729	1137
17	(G-F) / (GW)	1119	1320	1434	1162	1285
18	(G-F) / (GW)	1378	1580	1660	1340	1260
19	(GW)	930	1098	1211	972	1169
20	(GW)	1480	1746	1816	1457	1753
21	(G-F)	660	779	1091	880	887
22	(G-F)	1102	1300	1637	1320	1331
23	(GM)	551	650	1091	880	725
24	(GM)	913	1077	1637	1320	1088
25	(GM) / (GW)	673	794	1140	929	943
26	(GM) / (GW)	1387	1637	1711	1394	1415
27	(GM) / (G-F)	608	717	1091	880	810
28	(GM) / (G-F)	1032	1218	1637	1320	1214
29	(G-F) / (GW)	772	911	1148	929	1274
30	(G-F) / (GW)	1405	1658	1721	1394	1911

Table 3.6. Present and Computed Load Capacities.

3.12.1 Comparison between Present and Reese and O'Neill values

Reese and O'Neill (1988) method was intended for cohesionless Sand; therefore the computed results were increasingly conservative with an increase in gravel content.

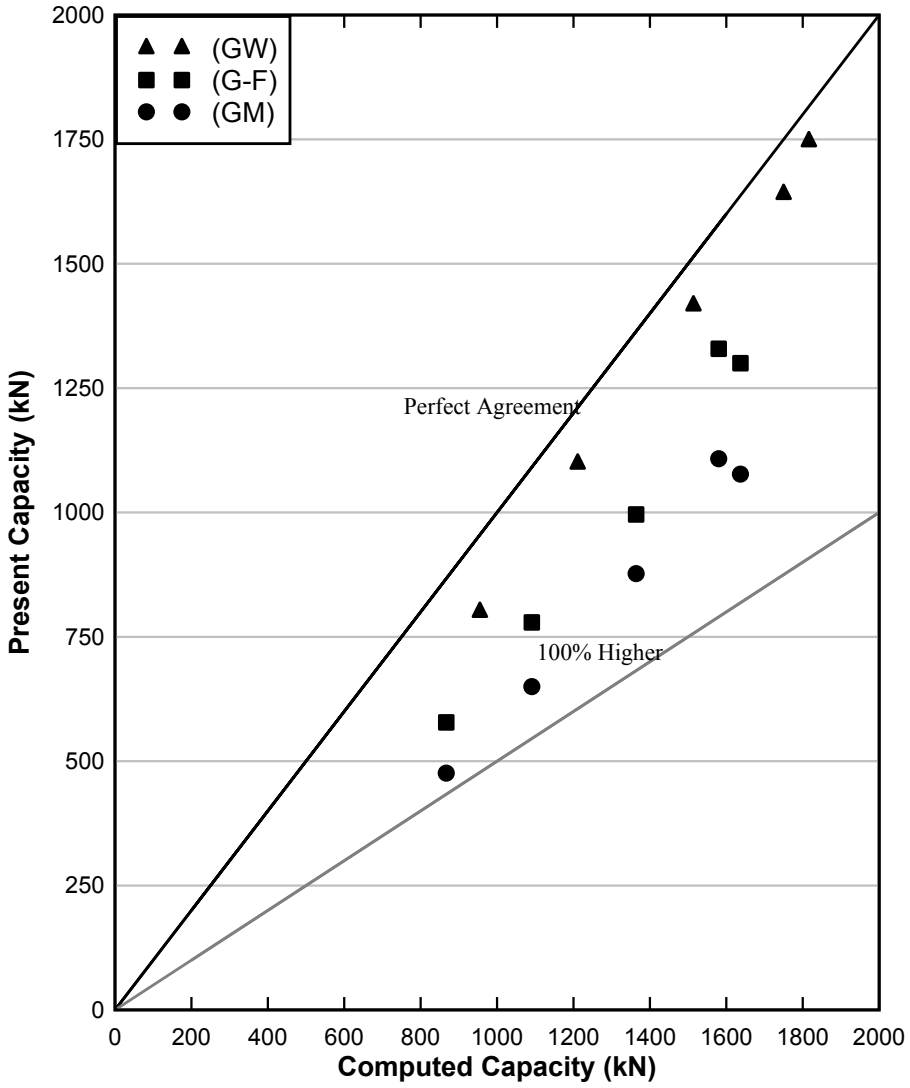

Figure 3.19. Comparison between Reese and O'Neill and Present capacities from numerical model, for homogenous gravelly soils.

On average, the Reese and O'Neill method revealed ultimate skin friction capacities that were 10% higher than the present capacities. For Gravel with traces of Fines (G-F) and Silty Gravel (GM), the Reese and O'Neill values for ultimate skin friction capacities were on average 35% and 60% higher than the present capacities, respectively.

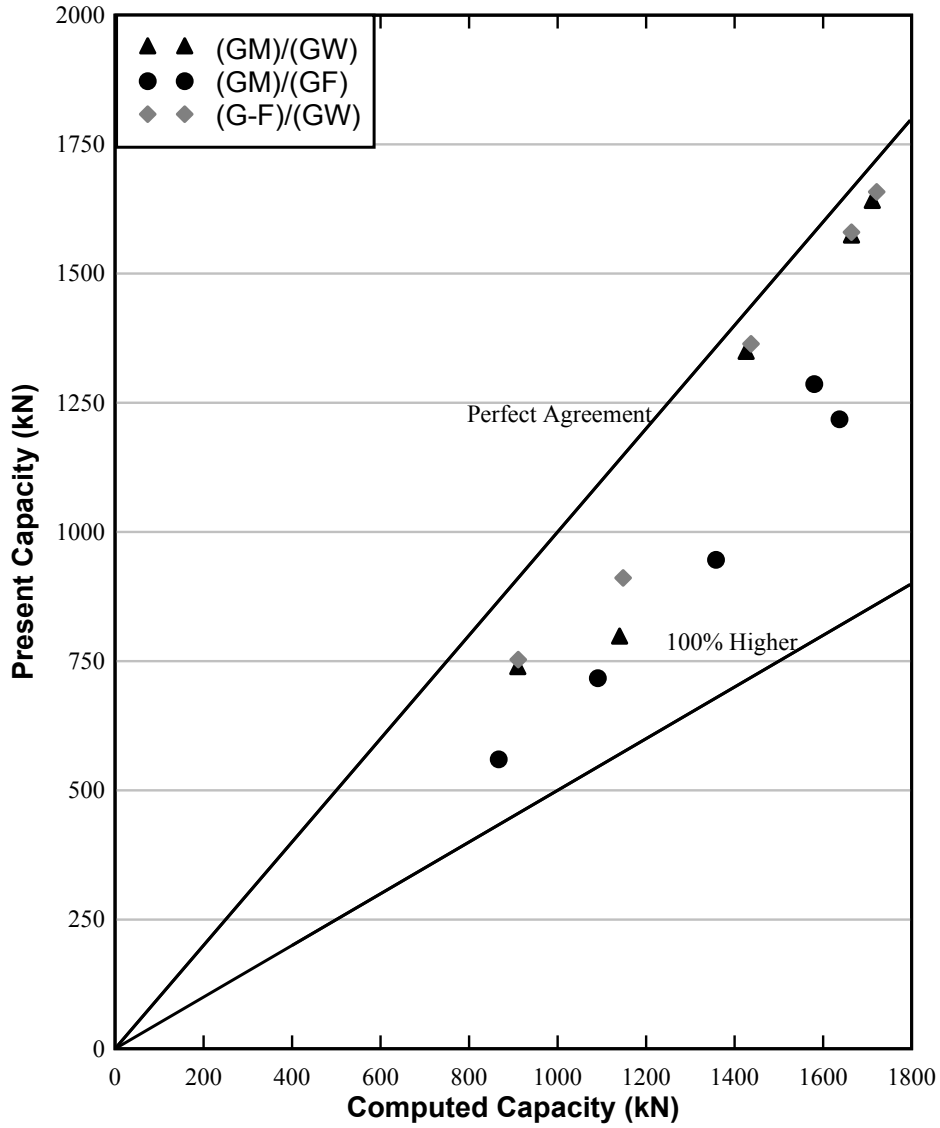

Figure 3.20. Comparison between Reese and O'Neill and Present capacities from the numerical model, for multi-layered gravelly soils.

The gap between present and computed capacities tends to narrow with an increase of gravel content, as shown in figure 3.19 and 3.20. A typical factor of safety of 2.0 would suggest exceedingly conservative values for well graded Gravel (GW) in the Reese and O'Neill method.

3.12.2 Comparison between Present and Hassan and O'Neill Values

Regarding the Hassan and O'Neill (1994) method, the computed ultimate skin friction capacities reveal exceedingly conservative values with an increase in gravel content. The method was essentially designed for sandy soils, thus the effect of dilation that results from the increase in gravel content was not accommodated in the equation, which may explain the conservative results recorded for Well Graded Gravel (GW), as shown in figure 3.21. On average, the computed capacities for Well graded Gravel (GW) were 12% lower than measured capacities, suggesting 23% discrepancy with that of the Reese and O'Neill method. A minimum factor of safety of 2 would unveil exceedingly conservative values. The computed ultimate skin friction capacities for Gravel with traces of Fines (G-F) and Silty Gravel (GM) were on average 8% and 29% higher than present capacities, respectively. Hassan and O'Neill method suggest moderately conservative results with a decrease in the gravel content, as revealed in Figure 3.21 and 3.22.

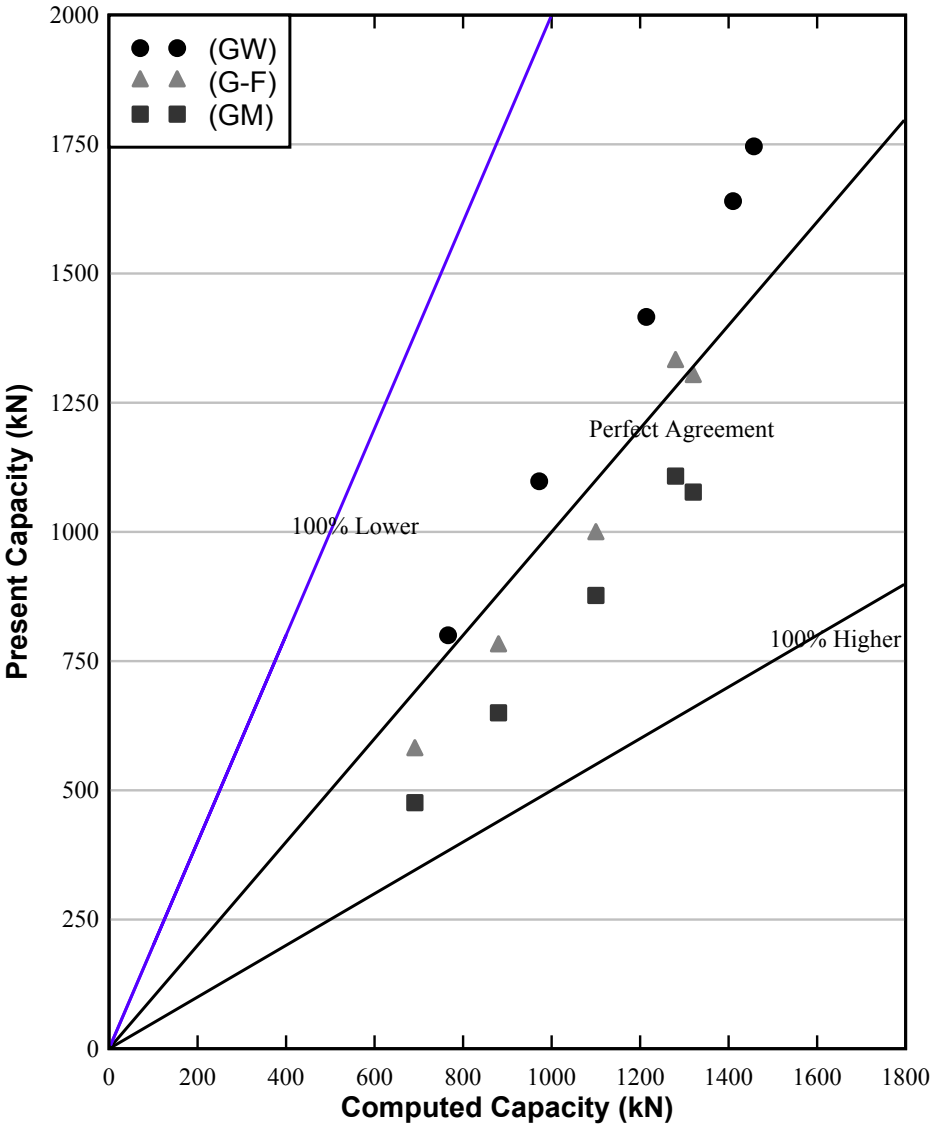

Figure 3.21. Comparison between the Hassan and O'Neill and the Measured Capacities from the numerical model for gravelly soils.

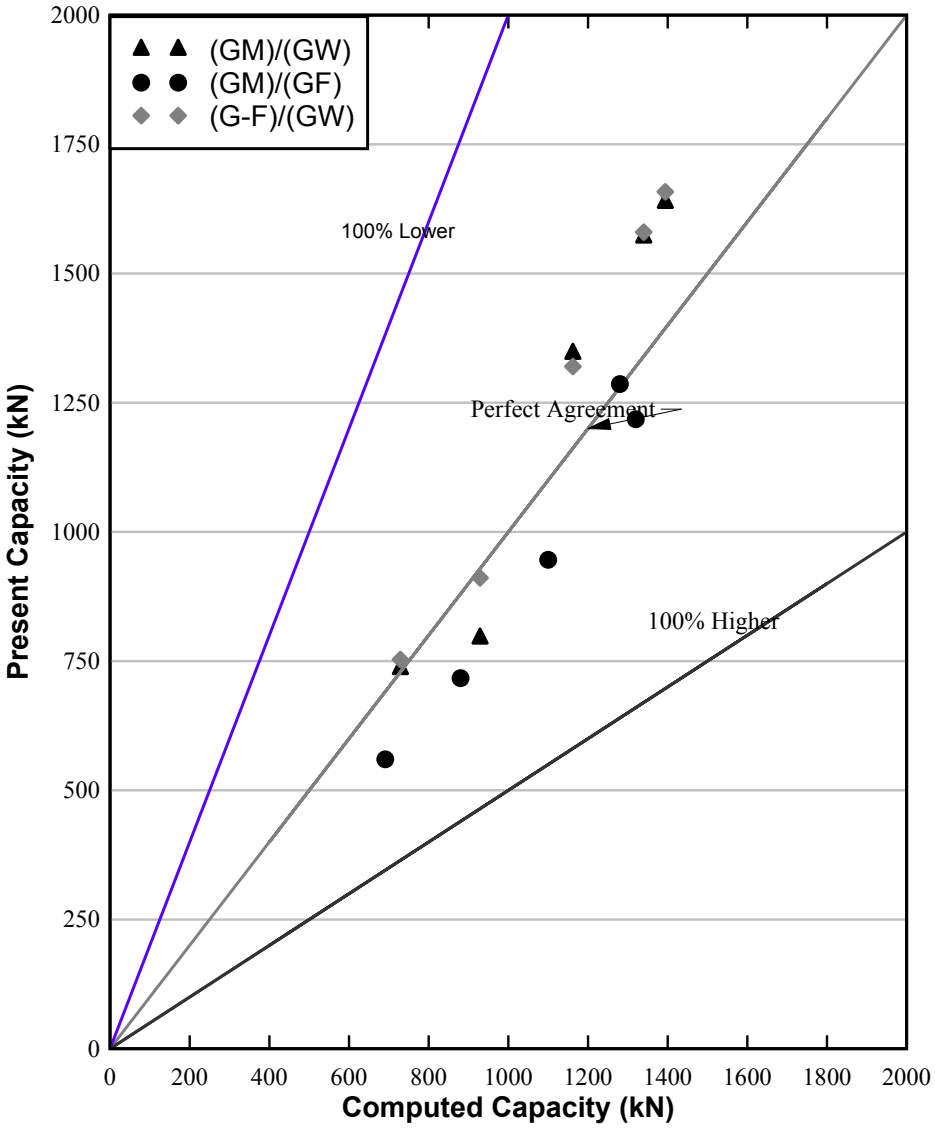

Figure 3.22. Comparison between the Hassan and O'Neill and the Present Capacities from the numerical model in multi layered gravelly soils.

3.12.3 Comparison between Present Values and adapted Kulhawy

The Kulhawy method was adapted by Rollins et al. (2005) to accommodate for gravelly soils. The authors suggested an empirical relationship to determine the lateral earth pressure K given by

$$K = 4.62e^{(-0.137z)}$$

The adapted Kulhawy method was used in this study to calculate the computed capacities. The results revealed consistency between different types of gravelly soils. For Well graded Gravel (GW), the computed ultimate skin friction capacities were on average 12% higher than present capacities. Both Gravel with traces of Fines (G-F) and Silty Gravel revealed similar results with a rise of 15% and 13% from the measured capacities, respectively.

For multi-layered gravelly soils, Silty Gravel (GM) overlying well graded Gravel gave the most conservative results with an average increase of 2.4% over the measured capacities.

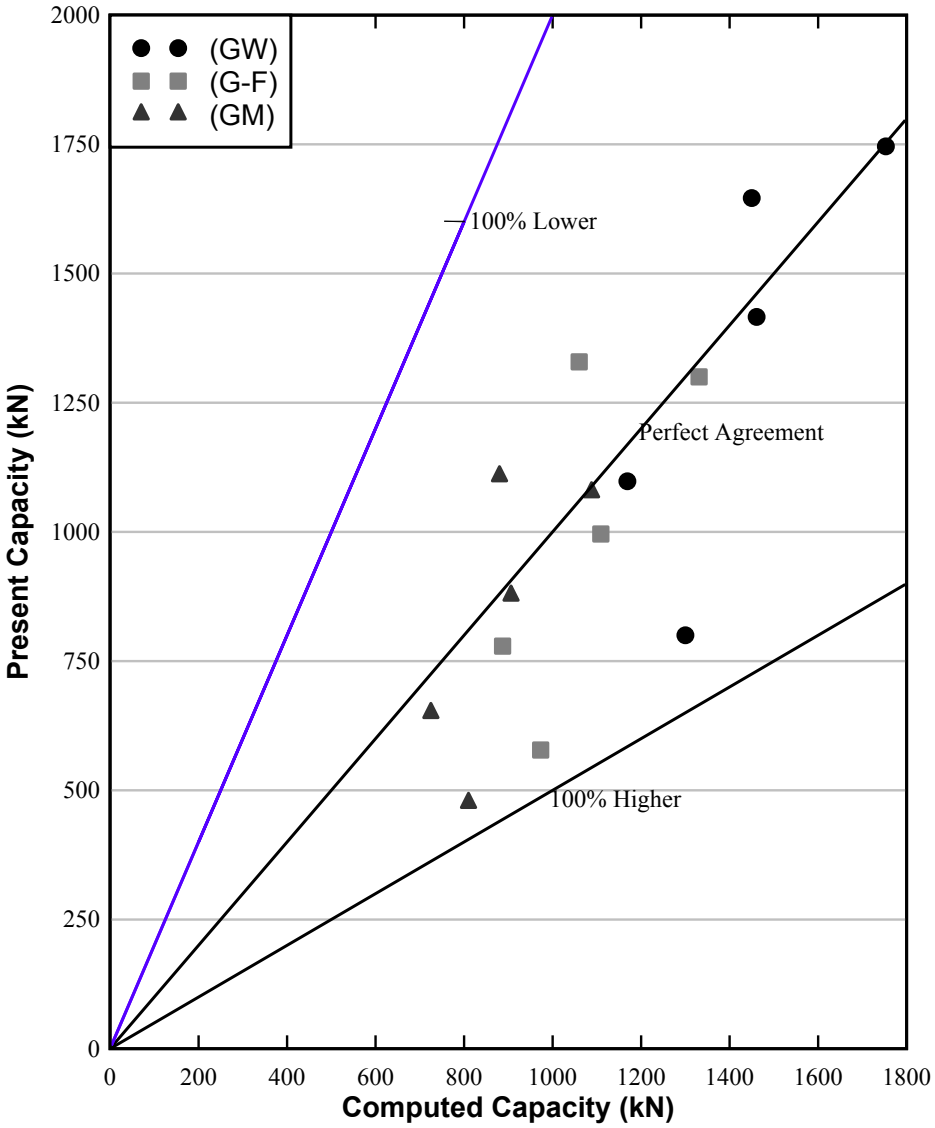

Figure 3.23. Comparison between the adapted Kulhawy method and the Present Capacities from the numerical model in gravelly soils.

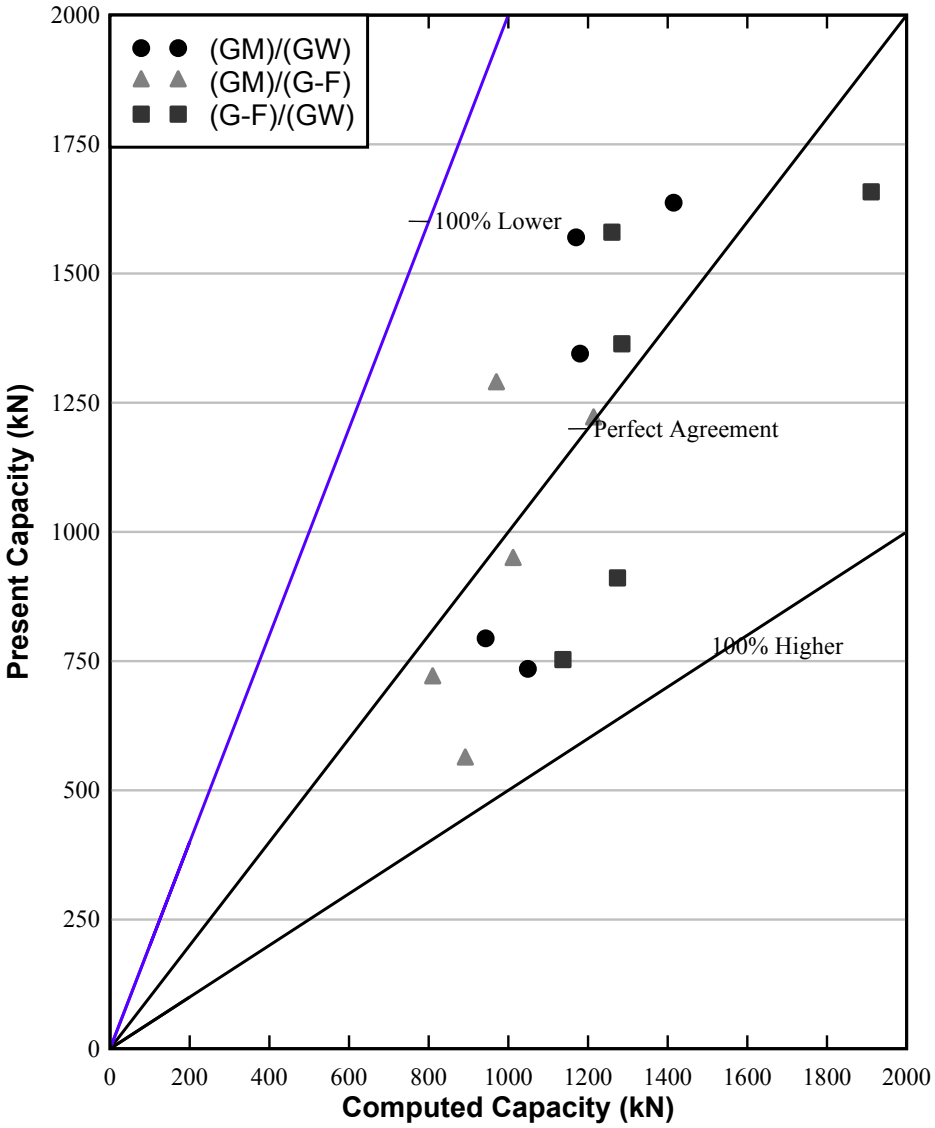

Figure 3.24. Comparison between the adapted Kulhawy method and the Present Capacities from the numerical model in multi layered gravelly soils.

Overall, the modifications to Kulhawy equation for gravelly soils, proposed by Rollins et al. (2005) for drilled shafts revealed moderately conservative results when compared with present capacities, as shown in Figure 3.23 and 3.24, respectively. The computed ultimate skin friction capacities reached to a maximum of 70% greater than the present capacities, which suggests that a minimum factor of safety of 2.0 would be acceptable in using this method for micropiles. However, there are also a number of cases, as shown in figure 3.23 and 3.24, where the present capacities are slightly greater than predicted by the equation, which suggests that a factor of safety of 2.0 would reveal conservative values.

3.12.4 Results

The results of this study indicate that modifications to the Reese and O'Neill (1988) and Hassan and O'Neill method (1994) are appropriate to bring about accurate computation for the ultimate skin friction capacity Q_s of micropiles in gravelly soils. The suggested modifications are based on data measured from the numerical model that was constructed in GEO5 Finite Element Method program for piles. Each modification is directly tied to the Davisson (1972) method used to determine the ultimate skin friction Capacity.

3.13 MODIFICATIONS TO DESIGN EQUATIONS

As revealed earlier in this chapter, the Reese and O'Neill equation multiplies the vertical effective stress by β factor to determine the ultimate unit skin friction on the shaft (see equation 5 of this present chapter).

Ten load tests were performed in the numerical model to evaluate micropiles embedded in Well Graded Gravel (GW) using the soil properties indicated in table 3.2. Load displacement curves were obtained. Backcalculated β values from previous and current load tests are plotted as a function of depth in Well graded Gravel, precisely where the gravel content exceeds 60%. As part of this analysis, the best-fit curves was determined for backcalulated β values using the software program **DPlot**.

Table 3.7. Backcalculated Beta (β) values captured for Well graded Gravel (GW).

Q_{L1}	Depth from Surface	Diameter	Backcalculated Beta
(kN)	(m)	(m)	β
678	10	0.2	0.49
1200	14	0.2	0.46
1396	16	0.2	0.41
930	14	0.16	0.45
1430	14	0.24	0.46
2000	27	0.25	0.19
650	8	0.25	0.62
520	12	0.12	0.46
840	28	0.14	0.12

Table 3.7 reveals the backcalculated values of β for Well graded Gravel, using the soil properties that are indicted in table 3.2.

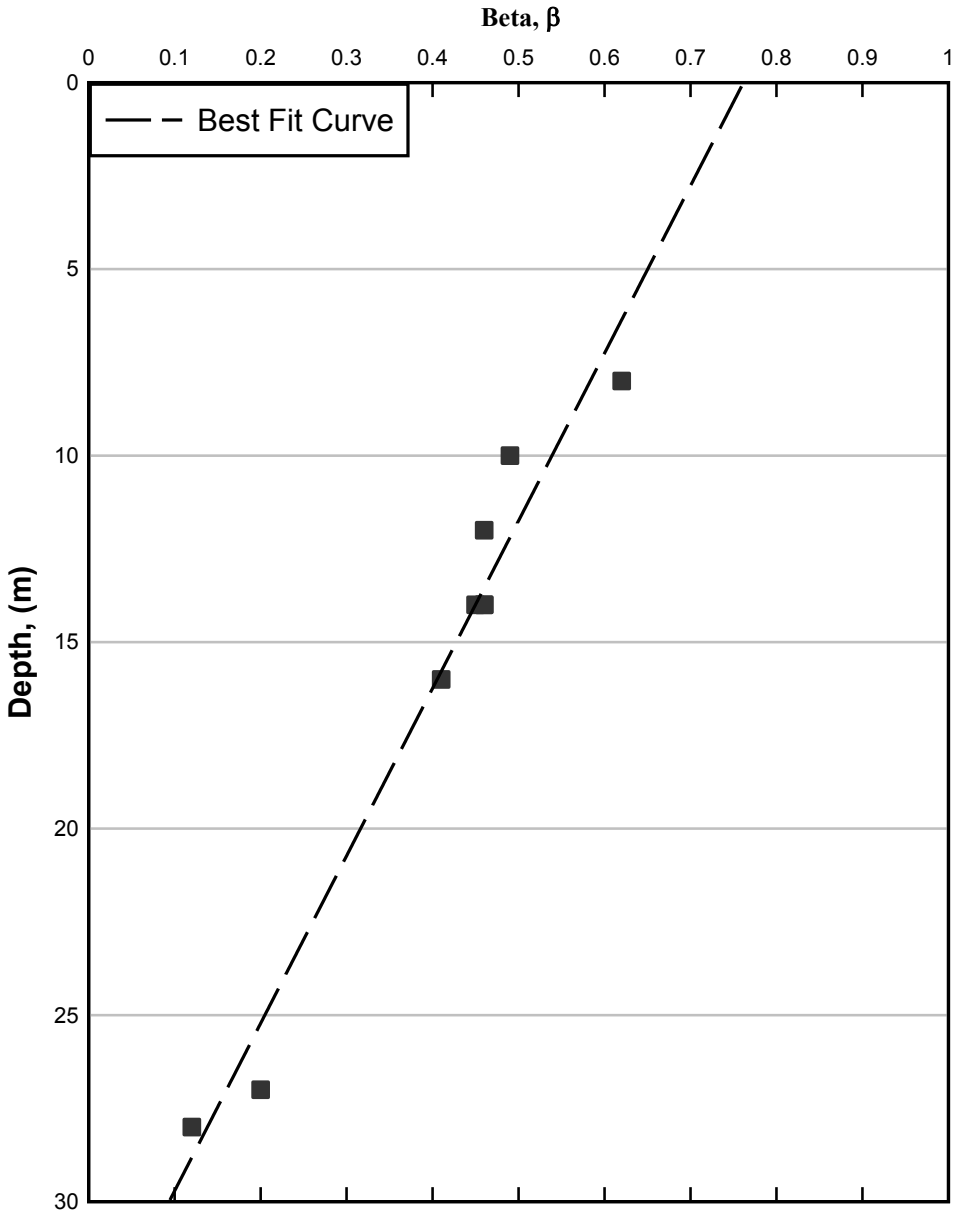

Figure 3.25. Back calculated β values from GEO5 FEM program for piles.

The best-fit curve for β revealed the following slope equation

$Z = 34.2 - 45\beta$

Where:

Z = depth below ground surface (m).

Solving for β gives

$\beta = 0.76 - 0.022Z$ Where $0.1 \leq \beta \leq 0.76$

Hirany and Kulhawy (2002) recommended that a factor of safety be chosen such that the design load is equal to or less than Q_{L1}. Given that all the back calculated values for β were measured from Q_{L1} , the Best-fit curve should be multiplied by 2, which is usually the minimum factor of safety chosen for deep foundations. Hence the Best curve fit for β becomes

$\beta = 1.52 - 0.044Z$ **Where $0.2 \leq \beta \leq 1.52$** (10)

3.14 DESIGN PROCEDURE

The adopted design procedure should respect the following conditions:

1) Diameter of micropile ≤ 0.30m (as indicated in the definition of a micropile by Bruce, 1994).
2) Micropile is fully bonded along the soil-shaft interface.
3) Uniform cross-sectional radius along the micropile's interface.
4) Micropile subject to direct axial compressive loading.
5) Grout poured under gravity head only (Type A micropile).

3.14.1 Computation of Ultimate Skin Friction for a single micropile embedded in cohesionless gravelly soils (Gravel content < 60%).

The Ultimate skin friction capacity Q_s is computed using the following equation:

$Q_s = \beta \times \sigma_z' \times A_s$

And the allowable $(Q_s)_{allowable}$ is given by

$(Q_s)_{allowable} = (Q_s)/F.S.$

Where F.S. = Factor of Safety.

Reese and O'Neill (1988) and Hassan and O'Neill (1994) methods for computing β in sand, as indicated in equation 6 and 7 of this present chapter, appear to be acceptable for micropiles embedded in gravelly soils where the gravel content does not exceed 60%, or the angle of

shearing resistance of soil ϕ is less than 35^0. The resulting values may generally be conservative but within the acceptable range. The adapted Kulhawy method suggested by Rollins et al. (2005) could be used as well with efficient results.

3.14.2 Computation of Ultimate Skin Friction for a single micropile embedded in cohesionless gravelly soils (Gravel content > 60%).

For gravelly soil layers where the gravel content exceeds 60%, β is calculated using equation (10) of this present chapter

$\beta = 1.52 - 0.044Z$ Where $0.2 \leq \beta \leq 1.52$

Once β is determined, the ultimate skin friction capacity (Q_s) and the allowable skin friction capacity $(Q_s)_{allowable}$ are then computed in the same fashion as indicated in 3.14.1.

3.14.3 Computation of Ultimate Skin Friction for a single micropile embedded in multi-layered gravelly soils.

For each layer the ultimate skin friction is computed using the appropriate β method for each soil type. The vertical effective stress is computed for each layer and the ultimate skin friction capacity for a single micropile becomes the summation

$Q_s = \sum \Delta Q_s = \sum \beta \times \sigma_z' \text{ x } A_s$

And the allowable Q_s is then given by

$(Q_s)_{allowable} = (Q_s)/F.S.$

It is important to mention that the Factor of Safety should be at least 2.0 for design calculations.

3.15 EXAMPLE

Given: A 0.20m micropile is to be constructed to a depth of 15m in the soil profile shown in figure 3.26. The soil profile consists of a 5m layer of Silty Gravel containing 15% of gravel content, overlying a 5m layer of Gravel with traces of fines that has 50% of gravel content, which in turn underlain by a 5m layer of Well graded Gravel containing over 60% of gravel size particles. Groundwater is located at a depth of 18m below the ground surface.

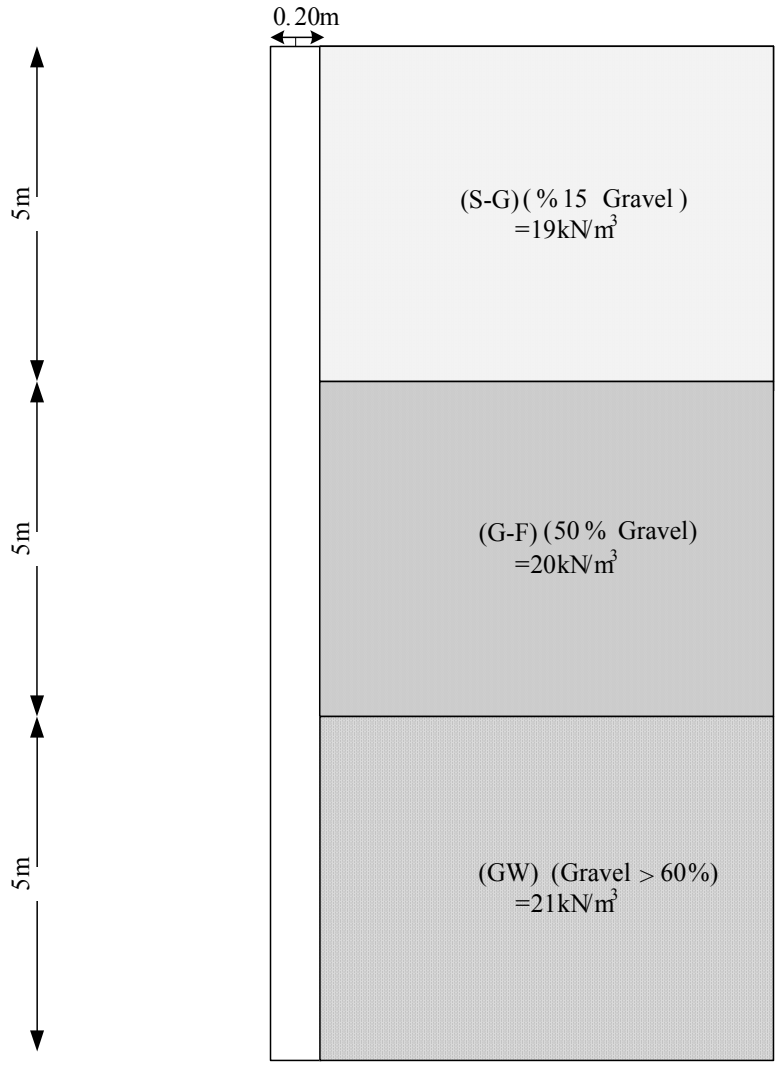

Figure 3.26. Dimensions of the micropile and the soil profile for the example.

Wanted: The ultimate skin friction capacity Q_s and the allowable carrying capacity $Q_{allowable}$.

Solution: For each given layer, the ultimate unit skin friction f_s is calculated using the appropriate Beta β method. The following table summarizes the skin friction calculations for each of the layers shown in figure 3.7

Table 3.8. Summary of skin friction calculations for example problem.

Soil Type	Depth Interval			σ'_z	A_s	ΔQ_s
	(m)	β	K	kN/m^2	m^2	kN
Sand with traces of Gravel	0-5	0.953		47.5	3.15	143
Gravel with traces of Fines	5-10	-	1.17	195	3.15	534
Well Graded Gravel	10-15	0.84		248	3.15	656
					Total Q_s	**1333**

$Q_s = \sum Q_s = \sum \beta * \sigma'_z * A_s$

For Sand with traces of Gravel, the adapted Kulhawy method used by Rollins et al. (2005) will be used:

$K = 4.62e^{(-0.137z)}$

$= 4.62e^{(-0.137(10))}$

$= 1.17$

Soil Pile friction was taken to be at 1.

For Well graded Gravel, equation 10 was taken to compute β:

$\beta = 1.52 - 0.044z$

$= 1.5 - 0.044(15)$

$= 0.84$

The ultimate Q_s is then given by

$(Q_s) = \sum Q_s = 143 + 534 + 656 = 1333kN$

And the allowable Q_s is computed by

$(Q_s)_{allowable} = Q_s/\text{Factor of Safety}$

Taken the factor of safety at 2,

$(Q_s)_{allowable} =$ **667kN**.

CONCLUSIONS

This report provided a general review on pile foundation and a detailed theoretical assessment on micropile design procedures and applications. A numerical model was developed to evaluate the skin friction of micropiles embedded in gravelly soils. The model was conducted through the software program GEO5 Finite Element Method for piles. The model was successfully validated with existing field test data. 30 load tests were then generated from the numerical model in order to assess the skin friction of micropiles embedded in gravelly soils. The load tests were performed in three types of gravelly soils, ranging from Silty Gravel (GM) to Well graded Gravel (GW). Typical load displacement curves were then developed. Present capacities were evaluated from the load displacement curves and then compared with capacities using equations proposed by Reese and O'Neill (1988), Hassan and O'Neill (1994) and the adapted Kulhawy method by Rollins et al. (2005). A parametric study on micropiles embedded in gravelly soils was carefully conducted. Based on the findings, the following conclusions could be made:

1. Ultimate skin friction capacity increases due to an increase in angle of shearing resistance of soil for micropiles embedded in gravelly soils.

2. Ultimate skin friction capacity increases due to an increase in gravel content for micropiles embedded in gravelly soils. This increase could be attributed to the rise in the lateral earth pressure caused by dilation of the soil and the roughness of the soil-skin interface.

3. With a constant diameter, increasing the length of a micropile embedded in gravelly soils, which automatically increases the slenderness ratio, results in a rise of the ultimate unit skin friction. In general, this rise seems to be less significant with an increase in both gravel content and angle of shearing resistance of soil.

4. With a constant length, increasing the diameter of the micropile embedded in gravelly soils, which automatically decreases the slenderness ratio, results in a rise of the ultimate unit skin friction.

5. The Reese and O'Neill equation (1988) and the Hassan and O'Neill equation (1994) were both designed for drilled shafts in sand, thus they both provided over conservative values for micropiles embedded in gravelly soils, given that a minimum factor of safety of 2.0 would be taken to compute the allowable skin friction capacity. Both equations become more conservative with an increase in gravel content.

6. The Reese and O'Neill (1988) equation and the Hassan and O'Neill (1994) equation are improved for micropiles (Type A) by using a modified proportionality coefficient β for soil layers where the gravel content exceeds 60% :

   $\beta = 1.52 - 0.044Z$ Where $0.2 \leq \beta \leq 1.52$

   A minimum factor of safety of 2 is used to compute the allowable skin friction capacity.

7. The adapted Kulhawy method provided by Rollins et al. (2005) for drilled shafts in gravelly soils can be safely used for micropiles embedded in gravelly soils for depths less than 20m.

RECOMMENDATIONS FOR FURTHER RESEARCH

Following the current study conducted in this present thesis, the following recommendations can be proposed for future research:

1) To examine the skin friction of micropiles embedded in cohesive soils.
2) To study the group efficiency of micropiles.
3) To study the effect of cyclic and seismic loads on micropiles.
4) To examine micropile/raft interaction.
5) To study the performance of micropiles under inclined axial load.

REFERENCES

American Association of State Highway and Transportation Officials (AASHTO) (1977). *Standard Specification for Highway Bridges*. Washington, DC, 469pp., Revised 1992.

Armour, T., and Groneck, P. (1998). "Micropile Design and Construction Guidelines and Implementation Manual." Report No. FHWA-SA-97-070, December 1998.

BCNYC (1991). Building Code of New York City.

Brown, D.A., Turner, J.P. and Custelli, R.J. (2010). "Drilled Shafts: Construction Procedures and LRFD Design." Report No. FHWA-NHI-016, May 2010.

Bruce, D.A. (1994). "Small-diameter cast-in-place elements for load bearing and in situ earth reinforcement." Chapter 6 in *Ground control and improvement* by P.P. Xanthakos, L.W. Abramson, and D.A. Bruce. John Wiley and Sons, 1994.

Bruce, D.A., and Juran, I. (1997a). "Drilled and Grouted Micropiles: State-of-Practice Review, volume 1: background, classifications, cost." Report No. FHWA-RD-96-016, July 1997.

Bruce, D.A., and Juran, I. (1997b). "Drilled and Grouted Micropiles: State-of-Practice Review, volume 2: Design." Report No. FHWA-RD-96-017, July 1997.

Bruce, D.A., Bruce, M.E.C., and Traylor, R.P. (1999). "High Capacity Micropiles – Basic Principals and Case Histories." GeoEngineering for Underground Facilities. Proc. of the 3rd National Conference of the Geo-Institute of the American Society of Civil Engineers. Geotechnical Special Publication No. 90, Urbana-Champaign, IL, June 13-17, pp. 188-199.

Bullivant, R.A., and Bradbury, H.W. (1996). Underpinning: a practical guide. Oxford, England: Blackwell Science Ltd.

Coduto, D.P. (2001) "Foundation Design: Principles and Practices." (2nd Edition). New Jersey: Prentice Hall.

Davisson, M.T. (1972). "High Capacity Piles." *Proceeding Lecture Series on Innovations in Foundation Construction*, Soil Mech. Div., Illinois Sec.-ASCE, Chicago, 81-112.

Dringenberg, G.E., and Craizer, W. (1990). "Capacidade de carga de micro-estacas injetadas." *IX COBRAMSEF – Congresso Brasileiro de Mecanica dos Solos e Engenharai de Fundacoes,* Salvador/BA, Novembro, 2(III), 325-332.

Fleming, W.G.K., Weltman, A.J., Randolph, M.F., and Elson, W.K. (1985). Piling engineering. First Edition. Surrey University Press. 380 pp. (Second Edition, 1992).

Frassetto, J.C. (2004). Performance of Micropiles. Montreal, Quebec. Concordia University.

GEO5 Geotechnical Software Suite, 2010. User's guide Manual Version 5.10. Los Angeles, California. Fine Ltd.

Gouvenot, D. (1975). "Essais de chargement et de flambement de pieux aiguilles." *Annales de l'Institut Technique du Bâtiment et des Travaux Publics, Comité Français de la Mécanique des Sols et des Fondations,* 334, December.

Hanna A., and Al-Romhein, R. (2008). "At-Rest Pressure of Overconsolidated Cohesionless Soil." *Journal of Geotechnical and GeoEnvironmental Engineering*, ASCE, March, pp.408-412.

Hanna, A., and Nguyen, T.Q. (2002). "An Axisymmetric Model for Ultimate Capacity of a Single Piles in Sand." *Journal of Soil Mechanics and Foundation Engineering,* Japan. 42 (2).

Hanna, A., and Nguyen, T.Q. (2003). "Shaft resistance of Single Vertical and Batter Piles in Sand Subjected to Axial Compression Loading." *Journal of Geotechnical and Environmental Engineering,* ASCE, 129 (3), 600-607.

Hassan, K.H., and O'Neill, M.W. (1994). Perimeter load transfer in drilled shafts in the eagle for formation. Geotechnical Special Publication No 38, Design and performance of deep foundations: piles and piers in soil and soft rocks; Edited by P.P. Nelson, T.D. Smith, and E.C. Klukey, ASCE, October, pp.229-244.

Hirany, A., and Kulhawy, F.H. (1989). "Conduct and interpretation of load tests on drilled shafts – part 1: axial compression." *Foundation Engineering: Current Principles and Practices (GSP 22),* Ed. F.H. Kulhawy, ASCE, New York, 1989, 1132-1149.

Hirany, A., and Kulhawy, F.H. (2002). "On the interpretation of Drilled Foundation Load Test Results." *Deep Foundations (GSP)*, Ed. M.W. O'Neill and F.C. Townsend, ASCE, Reston (Va), pp. 1018-1029.

Jeon, S., and Kulhawy, F.H. (2002). "Evaluation of axial compression behavior of micropiles." *Proceeding of a Specialty Conference – Foundation and ground improvement,* Blacksburg VI, ASCE, 460-471.

Jones, D.A., and Turner, M.J. (1980). "Load Tests on Post-grouted Micropiles in London Clay." *Ground Engineering*, 13 (6), 1980, 47-53.

Koreck, H.W. (1978). “Small diameter bored injection piles.” *Ground Engineering,* 11(4), 1978, 14-29.

Kulhawy, F.H. (1991). “Drilled shaft foundations.” *Foundation engineering handbook,* 2nd Ed., H.Y. Fang, ed., Van Nostrand-Reinhold, New York.

Kulhawy, F.H., and Mayne, P.W. (1990). “Manual on estimating soils properties for foundation design.” *Rep. No. EPRI EL-6800,* Electrical Power Research Institute, Palo Alto, Calif. 2-25.

Littlejohn, G.S. (1970). Soil anchors. Ground Engineering Conference. Institution of Civil Engineers, London, pp.32-44.

Littlejohn, G.S. (1980). Ground anchorage practice. ASCE Conference, Design and Performance of Earth Retaining Structures, Cornell University, Ithaca New York, June 18-21, pp. 692-733.

Lizzi, F. (1982). Static restoration of monuments. Sagep Publisher. Genova, Italy.

Lizzi, F., (1985). “Pali radice (root piles and reticulated pali radice).” Glasgow [Lanark]: Surrey University Press, 84-151.

Mascardi, C.A. (1982). “Design criteria and performance of micropiles.” *Symposium on Soil and Rock Improvement Techniques Including Geotextiles, Reinforced Earth and Modern Piling Methods,* Bangkok, December. Paper D-3.

Mayne, P.W. and Kulhawy, F.H. (1982). “Ko – OCR relationships in soil.” *Journal of the Geotechnical Engineering Division ,* ASCE, Volume 108, No GT6, June, pp 850-872.

MBC (1988). Michigan Building Code.

Meyerhof, G.G. (1976). “Bearing capacity and settlement of pile foundations.” *Journal of Geotechnical Engineering Division,* ASCE, Volume 102 (3), pp 195-228.

Pasternak, P.L. (1954). “A new method of analysis of an elastic foundation by means of two foundations constants.” *Gasudarstvennow Lzadatelstvo Literaturi po Stroiteslvui Arkhitekture,* Moscow, U.S.S.R.

Reese, L.C., and O’Neill, M.W. (1988). Drilled shafts: Construction procedures and design methods.” *Pub. No. FHWA-HI-88-042,* U.S. Dept. of Transportation, Washington, D.C., 564-565.

Rollins, K.M., Clayton, R.J., Mikesell, R.C., and Blaise, B.C. (2005). *“Drilled Shaft Side Friction in Gravelly Soils.”Journal of Geotechnical and Environmental Engineering*, ASCE, August 2005, pp 987-1003.

Tanahashi, H. (2007). “Pasternak Model Formulation of Elastic Displacements in the Case of a Rigid Circular Foundation.” *Journal of Asian Architecture and Building Engineering,* Vol. 6 (2007), No. 1 pp.167-173.

Thoburn, S., and Hutchison, F.C. (1985). Underpinning. Surrey University Press, London, England.

Tsukada, Y., Miura, K., Tsubokawa, Y., Otani, Y., and You, G.L. (2006). “Mechanism of Bearing Capacity of Spread Footings Reinforced with Micropiles.” *Japanese Geotechnical Society*, Vol. 46, No.3, June 2006, pp 367-376.

Winkler, E. (1867). Die Lehre Von Elasticitaet Und Festigkeit. 1st Edition., H. Dominicus, Prague.